DEFENSE DOCUMENTATION CENTER

FOR

SCIENTIFIC AND TECHNICAL INFORMATION

CAMERON STATION, ALEXANDRIA, VIRGINIA

TRANSLATION

CYCLIC STRENGTH OF METALS
(SELECTED ARTICLES)

FOREIGN TECHNOLOGY DIVISION

AIR FORCE SYSTEMS COMMAND

WRIGHT-PATTERSON AIR FORCE BASE

OHIO

411491
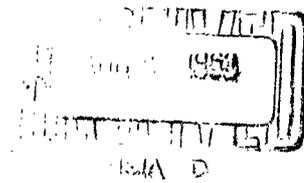
UNEDITED ROUGH DRAFT TRANSLATION

CYCLIC STRENGTH OF METALS (SELECTED ARTICLES)

English Pages: 71

SOURCE: Russian Book, Tsiklicheskaya Prochnost' Metallov, Akademiya Nauk SSSR, Institut Metallurgii im. A. A. Baykova, Moskva, 1962, pp. 123-133, 233-266

S

TABLE OF CONTENTS

INVESTIGATION OF THE POSSIBILITY OF APPLYING THE
ACCELERATED METHOD OF DETERMINING FATIGUE STRENGTH
UNDER CONDITIONS OF AN ASYMMETRIC LOADING CYCLE AND
WITH VARIOUS PRODUCTION TREATMENTS

M.A. Yel'yasheva

The hypothesis of energy similarity between fatigue failure and melting of metals provides a basis for applying the accelerated method for determination of fatigue strength. This method was proposed by V.S. Ivanova [1, 2].

On the basis of V.S. Ivanova's data, the cyclic constant α is an approximate constant. Therefore, the possibility of using the accelerated method reduces to establishment of the constancy of the critical number of cycles N_k on varying different factors.

The accelerated method of fatigue testing was confirmed in References [1, 2] for pure metals and certain alloys only in a symmetrical loading cycle. The present study cites the results of determination of the critical number of cycles for certain alloys in symmetric and asymmetric loading cycles on varying the state of the surface layer, the welding procedure and other technological factors.

Our data are statistical in nature and are based on the systematization and evaluation of fatigue curves obtained earlier on study of the influence of procedure on strength. The results make no pretense whatever to complete solution of the problem and we regard them as preliminary.

Fatigue curves obtained on testing specimens of aluminum, mag-

nesium and titanium alloys, alloy steels and several other alloys were evaluated.

The tests were conducted on various machines and under various schemes of specimen loading and cycle asymmetry (Fig. 1).

Circular rotating specimens fixed at both ends were tested on an NU machine (NIKIMP design); a constant bending moment was applied to the center section of the specimen. The stress on the surface of the specimen varied in the range from $\pm\sigma_{max}$ in the process, i.e., in accordance with a symmetric cycle.

Flat specimens were tested on a Shenk-Erlinger pulser by applying an axial load varying in the range from σ_{max} to σ_{min} with the constant ratio $\sigma_{min}:\sigma_{max} = 0.1$. The test results obtained on the pulser correspond to a well-defined asymmetric loading cycle with a constant asymmetry coefficient.

Tests were conducted on an SU machine by bending the ends of flat cantilevered specimens with a constant vibration amplitude (at the point of load application). The design of the machine permits conducting tests on the basis of symmetric and asymmetric (more precisely, pulsating) loading cycles.

Thus, utilization of the test results obtained on these three types of machines enabled us to check the proposed method not only in a symmetric loading cycle, but also in an asymmetric tension cycle.

The loading schemes, which are indices of cycle asymmetry in accordance with Fig. 1, are pointed out in the fatigue curves shown below.

In view of the absence of the required data for obtaining computed values of the critical fatigue stress (σ_k) and the critical number of cycles (N_k) for the majority of materials considered, determination of these values was carried out not by calculation, but directly from

- 2 -
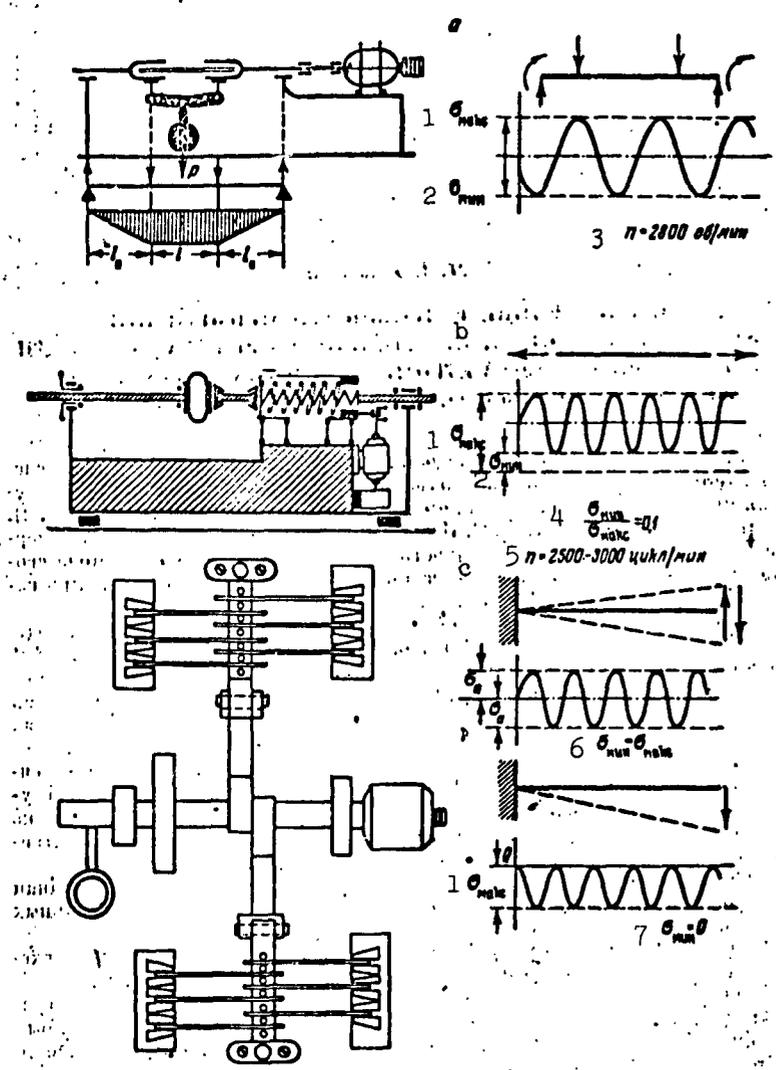
Fig. 1. Loading schemes and cyclic stress diagrams of specimens. a) On NU machine (bending test during rotation of specimen); b) on resonance type Shenk-Erlinger pulser; c) on SU machine (bending test on cantilevered specimens). 1) σ_{max}; 2) σ_{min}; 3) n = = 2800 rpm; 4) $\sigma_{min}/\sigma_{max}$ = 0.1; 5) n = 2500-3000 cycles/min; 6) $\sigma_{min} = \sigma_{max}$; 7) σ_{min} = 0.

experimental fatigue curves. The values of the cyclic failure constant α_σ for pure metals, which were cited in studies by V.S. Ivanova, were employed for this purpose. The cyclic constant, as is shown in the

- 3 -

above study, varies only very slightly; therefore, the values of the cyclic constant for the pure metals on whose basis the given alloy is produced were taken for the various alloys.

TABLE 1

Cyclic Constant for Certain Alloys

1 Материал	$\sigma_o - \sigma_{\scriptscriptstyle H} = \sigma_{\scriptscriptstyle W}$
2 Магниевый сплав МА8	6,5
3 Технический титан ВТ1Д	6,0
4 Алюминиевые сплавы (Д16Т, Д19Т, В-95, В-92)	7,0
5 Никелевый сплав ЭИ-437Б	6,5
6 Стали 1Х18Н9Т, ЭИ-659, ЭИ-654, 30ХГСА, СН3, СТ3	6,0

1) Material; 2) MA8 magnesium alloy;
3) VTID commercial titanium; 4) alu-
minum alloys (D16T, D19T, V-95 and
V-92); 5) EI-437B nickel alloy; 6)
1Kh18N9T, EI-659, EI-654, 30KhGSA,
SN3 and ST3 steels.

The values assumed for the cyclic constant and the corresponding difference between the critical stress σ_k under which failure occurs after N_k cycles and the fatigue strength σ_w (on the basis of 10^7 cycles) in tension and bending are shown in Table 1.

The critical fatigue stress was determined on the basis of the experimental value of the fatigue strength σ_w after which the value of the corresponding critical number of cycles N_k was found from the fatigue curve. Then a comparison of the values obtained for the critical number of cycles N_k as a function of cycle asymmetry, various technological factors and so forth was made for the given material. Coincidence of the critical number of cycles under different test conditions and treatment procedures may, in first approximation, serve as a confirmation and basis for adopting the accelerated method for determination of fatigue strength. Data on the influence of various factors on the critical number of cycles are cited below.

Influence of cycle asymmetry. In many cases, tests on the basis of an asymmetric loading cycle correspond closely to the real operating conditions of the designs. Moreover, a loading scheme on the basis of an asymmetric cycle is the only one possible for cyclic tension tests on sheet materials, welded, bolted, glued and riveted joints and in many other cases. Therefore, confirmation of the applicability of the proposed hypothesis under conditions of an asymmetric loading cycle attracts much practical interest.

Figure 2 shows the fatigue curves for a number of materials, which were obtained in symmetric bending (specimens 10 mm in width) and asymmetric tension (specimens 30 mm in width) tests. Comparison of these curves attests to the agreement of the critical number of cycles for one and the same metal in symmetric and asymmetric loading cycles. Such a comparison was made for the magnesium alloy MA8, commercial titanium, alloy EI-654 and the aluminum alloy D16T, as well as welded joints formed by different methods in several of these materials.

Figure 3 compares the experimental data obtained on the same machine on testing in accordance with symmetric and pulsating loading cycles for alloy V-92 in cantilevered bending. These data also confirm the constancy of the critical number of cycles for a given material irrespective of cycle asymmetry.

Influence of state of material. Figure 4 cites the results of testing the aluminum alloy D19 in the annealed and age-hardened state (with and without subsequent heat treatment).

As we see from the data presented, the critical number of cycles remains the same, $3.5 \cdot 10^5$, irrespective of the state of the material and the fatigue strengths (which differ one from another).

Influence of surface layer. It is known that fatigue resistance
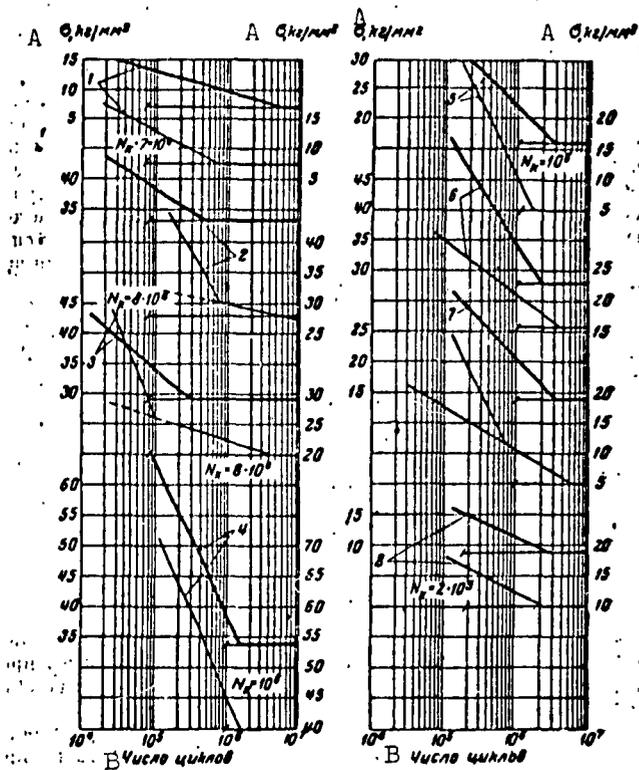
Fig. 2. Fatigue curves for symmetric (bending, left-hand scale) and asymmetric (tensioning, right-hand scale) loading cycles of various sheet materials 1.5 mm thick. 1) Alloy MA8; 2) commercial titanium VT1D; 3) same, argon-shielded arc welding without filler; 4) EI-654 steel; 5) same, argon-shielded arc welding with filler; 6) same, reinforcement removed (without stress concentration); 7) same, resistance seam welding; 8) D16T alloy.

A) σ, kg/mm^2; B) number of cycles.

varies essentially as a function of the state of the surface layer; in principle, this is linked with the method of surface treatment.

Figure 5 shows the fatigue curves obtained on 30KhGSA steel specimens (20 mm in diameter) after turning in which tools with different back-rake dressing angles were used [3]. The fatigue strengths varied from 36 to 57 kg/mm^2, while the critical number of cycles remained 10^6 for all procedures.

- 6 -
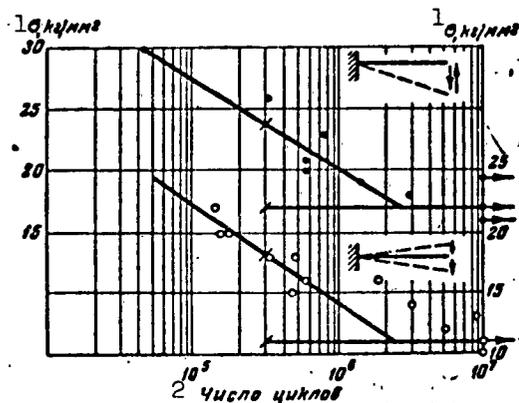
Fig. 3. Fatigue curves in symmetric (left-hand scale) and pulsating (right-hand scale) loading (bending) cycles for V-92 alloy ($\delta = 1.5$ mm, $B = 10$ mm). 1) σ, kg/mm^2; 2) number of cycles.

Figure 6 cites the fatigue curves of V-95 alloy specimens with different surface layer states produced as a result of applying various finishing operations. As the above data indicate, the fatigue strength may fluctuate in a rather wide range depending upon the method of working; its magnitude may increase by 40-50% as compared with the initial state. Here the critical number of cycles remains unchanged at $2 \cdot 10^5$.

The fatigue curves shown in Fig. 6 by the solid lines represent averaged experimental data; the inclined branches of the fatigue curves based on the lower and upper points of the experimental data are plotted by broken lines on the same diagram. In this case, (considering that the critical number of cycles N_k and the cyclic failure constant should remain unchanged) the theoretical values of the fatigue strengths obtained in accordance with the proposed method are denoted by broken horizontal lines.

As we see from the data under consideration, the theoretical

- 7 -

values of the fatigue strengths are entirely within dispersion range of the experimental data.

Influence of Welding. The possibility of adopting the proposed method was also checked against experimental data obtained from fatigue tests on welded-joint specimens. As an example, data on welded joints between titanium and EI-654 steel are shown above (see Fig. 1), while data for SN3 steel and type V-92 aluminum alloy are shown in Figs. 7 and 8. It was shown on the example of EI-654 steel that the value of N_k remains the same for joints produced by different welding procedures (argon-shielded and seam welding) as for the base material; nor does removal of reinforcement after welding with filler wire reflect on the value of N_k. The value may vary on welding with filler wire that differs in chemical composition from the material being welded (Fig. 8).

Table 2 shows the critical number of cycles for various materials, which were obtained as a result of evaluating a number of fatigue curves. The values of N_k for commercial titanium agree well with theoretical data for pure titanium. For aluminum alloys, alloy steels, and alloy MA8, the experimental values of N_k differ from the theoretical for the corresponding pure metals.

Let us note that the N_k values obtained for alloy V-95 agree well with the experimental data cited by V.S. Ivanova [2] for the same material in other states. Such coincidence was not obtained for certain other materials; thus, for example, according to V.S. Ivanova, $N_k = 2 \cdot 10^5$ for steels containing from 0.1 to 0.9% of C in various states during rotational bending tests, while according to our data, $3N_k = 3.5 \cdot 10^5$ for flat steel specimens.

There is a discrepancy in the values of N_k, which were obtained for 30KhGSA steel; thus, according to the data that we evaluated from
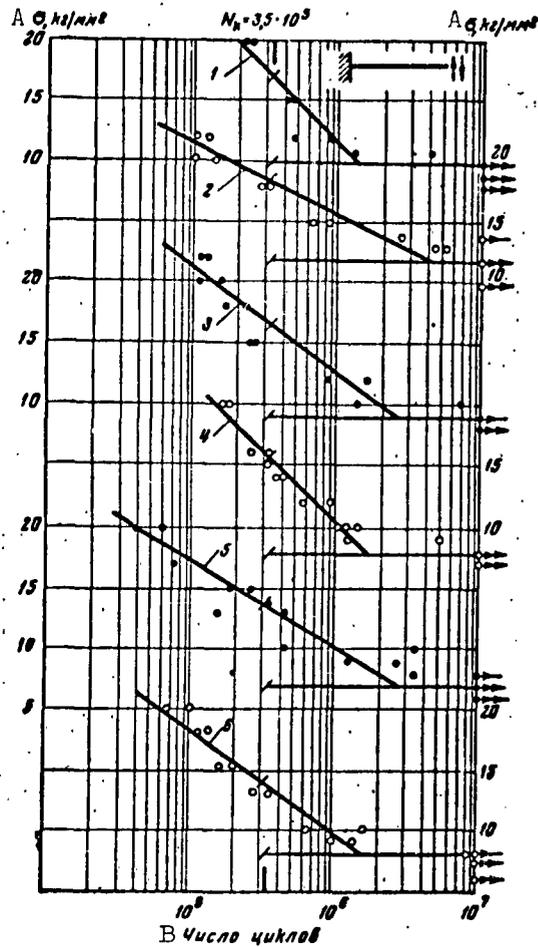
Fig. 4. Fatigue curves of D19 alloy with thickness of 2 mm in different states. 1) Annealed; 2) age-hardened; 3) annealed with subsequent quenching and aging; 4) age-hardened with subsequent quenching and aging; 5) argon-shielded arc welding (of annealed material) with subsequent quenching and aging; 6) same (age-hardened material). A) σ, kg/mm^2; B) number of cycles.

fatigue tests of specimens 20 mm in diameter in rotational bending (see Fig. 5), $N_k = 10^6$; for heat-treated specimens 7.5 mm in diameter, however, the values of N_k fluctuate in the range from 2 to $3 \cdot 10^5$. It is possible that these discrepancies are linked with the in-

- 9 -
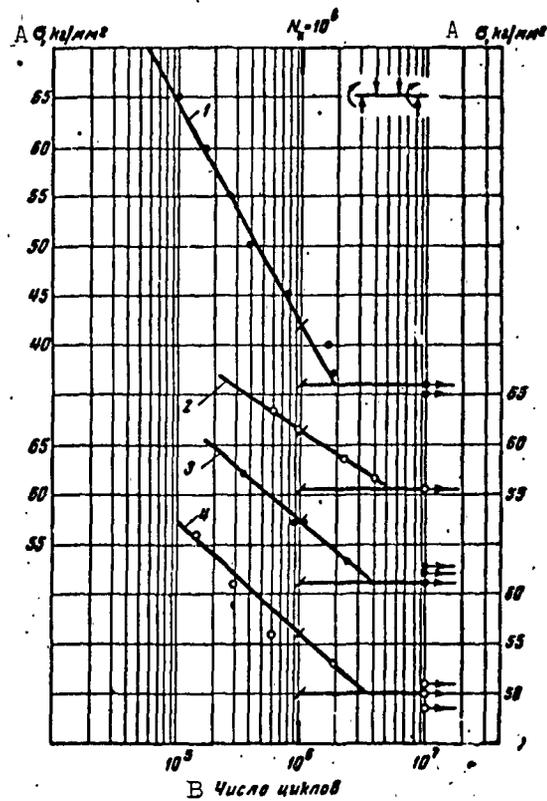
Fig. 5. Fatigue curves of 30KhGSA
steel after turning with tools of
various back-rake angles. 1) $\sigma_{-1} =$
$= 36.2$ kg/mm^2, $\gamma = 10^{\circ}$; 2) $\sigma_{-1} = 57.4$
kg/mm^2, $\gamma = -50^{\circ}$; 3) $\sigma_{-1} = 55$ kg/mm^2,
$\gamma = -25^{\circ}$; 4) $\sigma_{-1} = 50$ kg/mm^2, $\gamma = 0^{\circ}$.
A) σ, kg/mm^2; B) number of cycles.
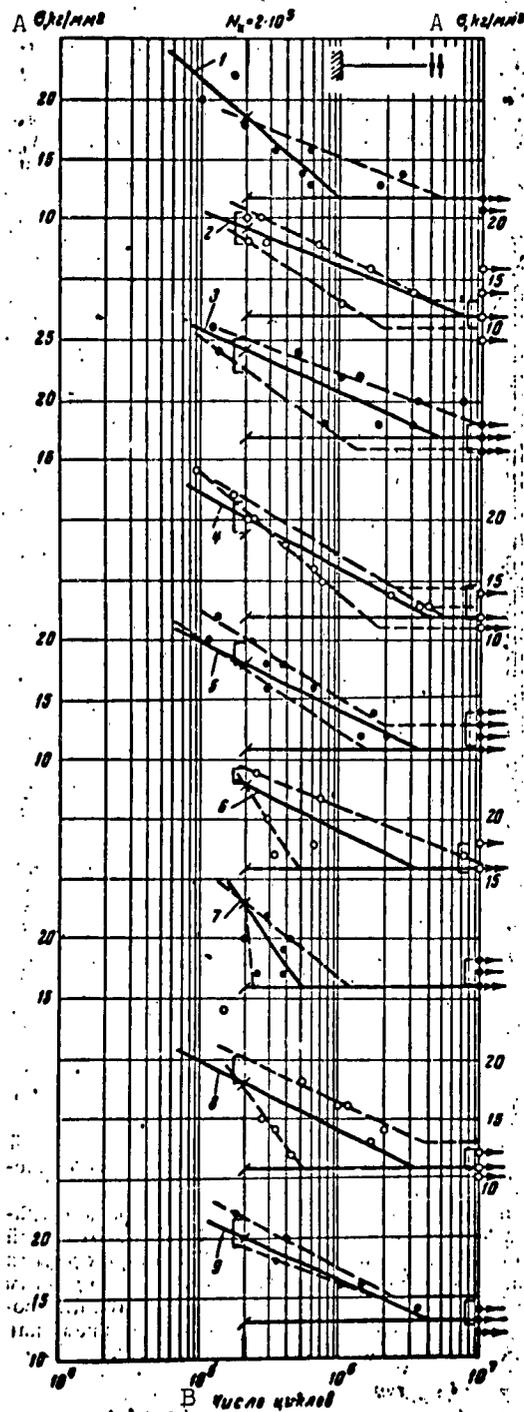
Fig. 6. Fatigue curves of ex-
truded-panel specimens of
V-95 alloy 2 mm thick. 1)
Without treatment; 2) hydro-
polishing on one side; 3)
same, on two sides; 4) durix;
5) durix and buffing with
abrasive paper on two sides;
6) durix and hydropolishing
on two sides; 7) durix and
hydroanodizing on two sides;
8) chemical milling on one
side; 9) chemical milling and
hydropolishing on one side.
A) σ, kg/mm^2; B) number of
cycles.
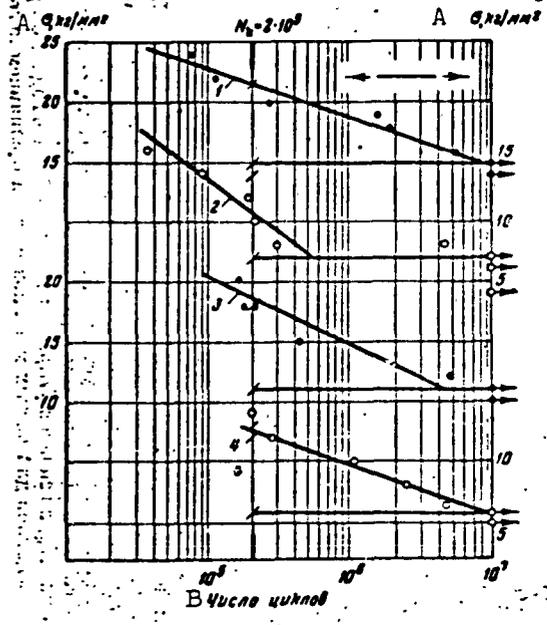
Fig. 7. Fatigue curves of type V-92 aluminum alloy (asymmetric tensioning). 1) Base metal; 2) argon-shielded arc welding with filler (procedure 1); 3) same, reinforcement removed; 4) argon-shielded arc welding (procedure 2). A) σ, kg/mm^2; B) number of cycles.
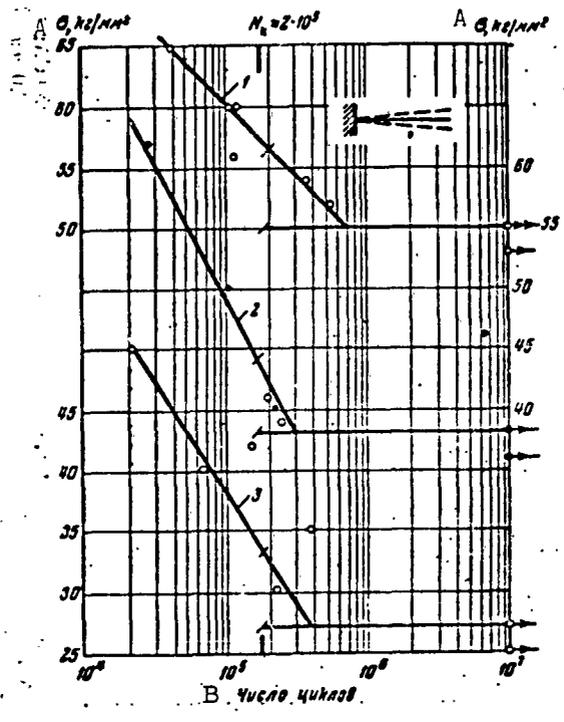
Fig. 8. Fatigue curves of base material and welded joints of SN3 specimens (symmetric cycle, SU machine). 1) Base material; 2) argon-shielded arc welding; 3) same, after heat treatment. A) σ, kg/mm^2; B) number of cycles.

fluence of the scaling factor — the more so because these results of cantilever bending tests of flat specimens 2 mm in thickness agree with the test results of specimens 7.5 mm in diameter.

It is necessary to note that the natural scattering of the experimental data, which is particularly wide in investigation of technological factors, makes it possible for the slope of the fatigue curve to vary; this makes it difficult to establish an accurate value for the critical number of cycles. Due to the absence of required data (melting point, specific heat and so forth), it is impossible to confirm the values of N_k for a number of materials by calculation

TABLE 2

Values Obtained for Critical Number of Cycles

1) Метал	$N_к$	2) Сплав	3) Цикл	
			симметричный $N_к$ 4)	асимметричный $N_к$ 5)
6) Магний	1,1·10⁶	МА8	7·10⁶	7·10⁶
7) Титан	7,1·10⁶	10) ВТ1Д, лист и сварные соединения . . .	8·10⁶	8·10⁶
		11) Сталь 3 (σ = 40 кг/мм²), лист (δ = 1,2 мм) шлифованный	4·10⁶	4·10⁶
		12) 1Х18Н9Т, точечная сварка	10⁶	6·10⁶
8) Железо	2·10⁶	13) ЭИ-654, лист и сварные соединения . . .	10⁶	10⁶
		14) 30ХГСА (σ = 120 кг/мм²) с разным состоянием поверхностного слоя		3·10⁶
		15) СН3, лист (δ = 2 мм) сварные соединения	2·10⁶	—
		16) Д16Т, лист (δ = 2 мм) и сварные соединения, в том числе с точечной сваркой	2·10⁶	2·10⁶
		17) В-95, прессованная панель с разным состоянием поверхностного слоя	2·10⁶	
9) Алюминий	2,3·10⁶	18) Д19, лист в разных состояниях (отожженный, нагартованный, термообработанный и т. д.) и сварные соединения	3,5·10⁶	
		19) В-92 сварные	3·10³	

1) Metal; 2) alloy; 3) cycle; 4) symmetric N_k; 5) asymmetric N_k; 6) magnesium; 7) titanium; 8) iron; 9) aluminum; 10) VT1D, sheet and welded joints; 11) steel 3 $(\sigma = 40 \text{ kg/mm}^2)$, sheet $(\delta = 1.2 \text{ mm})$ ground; 12) 1Kh18N9T, spot welding; 13) EI-654, sheet and welded joints; 14) 30KhGSA $(\sigma = 120 \text{ kg/mm}^2)$ with different surface layer states; 15) SN3 sheet $(\delta = 2 \text{ mm})$, welded joints; 16) D16T, sheet $(\delta = 2 \text{ mm})$ and welded joints, including spot welding; 17) V-95, extruded panel with different surface layer state; 18) D19, sheet in various states (annealed, age-hardened, heat-treated and so forth) and welded joints; 19) V-92, welded.

without additional investigations.

CONCLUSIONS

1. The use of the accelerated method to determine fatigue resistance is promising for solution of a series of technological problems.

2. A satisfactory coincidence of the critical number of cycles occurs on comparing the fatigue curves of specimens with different production treatment (for one and the same material).

3. The value of N_k for alloys in isolated cases does not coincide

with the critical number of cycles for the pure metals due to the influence of the alloying elements on the physical constants (C_p, T_s, E and so forth) [2].

4. Other conditions similar, cycle asymmetry does not exert a noticeable influence on the quantity N_k.

5. The data obtained may be regarded only as preliminary. The possibility of the practical use of the proposed method is limited for the majority of alloys by the absence of verified fatigue criteria, as well as specific data on the limitations and permissible fields of application of the method (the scaling factor, test conditions and so forth).

Studies should be continued in this direction by setting up special investigations and statistical evaluation of the experimental data available in various organizations.

REFERENCES

1. V. S. Ivanova, Izv. AN SSSR, OTN [Bull. Acad. Sci. USSR, Div. Tech. Sci.], No. 1, 1960.

2. V. S. Ivanova, Zavodskaya laboratoriya [Industrial Laboratory], No. 5, 1960.

Manu-script Page No.	[List of Transliterated Symbols]
1	к = k = kriticheskiy = critical
2	НУКИМП = NIKIMP [unlisted]
3	макс = maks = maksimal'nyy = maximum
3	мин = min = minimal'nyy = minimum

INFLUENCE OF THE EXTERNAL MEDIUM ON FATIGUE RESISTANCE

FUNDAMENTAL FACTORS ON INVESTIGATION OF THE EFFECT OF THE EXTERNAL MEDIA ON FATIGUE RESISTANCE

T.V. Karpenko

The time required to give rise to the phenomena of both static and cyclic fatigue is the fundamental factor where the external working media act on the mechanical characteristics of solids. Actually, the changes in the mechanical properties of solids under the influence of the external media that are caused by corrosion, diffusion, radiation, erosion and cavitation processes usually require considerable time. Therefore, the active external media almost always influence the long-term strength and cyclic fatigue of solids.

A rather short time is required to change the mechanical properties of solids in media whose influence on the solids is based on a considerable adsorption reduction in the level of surface energy. Certain metallic melts that reduce by several times the plasticity of metals in a deformation process that is carried out at a speed of a few millimeters per minute belong to these media. This is confirmed by the experiments of P.A. Rebinder and V.I. Likhtman (IFKh of the Acad. Sci. USSR, Moscow) with metallic monocrystals and M.I. Chayevskiy (IMAShiA of the Acad. Sci. Ukrainian SSR, L'vov) with large-diameter steel specimens.

Furthermore, media based on the action of hydrogen belong to the fast-acting media; this is explained by the high displacement rate of hydrogen inside the material. The proton gas generated as a result of the action of a medium that causes a metal to absorb hydrogen,

fails to provoke changes in the chemical properties of the materials only on deformations that proceed at extremely high rates, for example, deformations caused by impact loadings.

Thus, an influence of the external working media on fatigue resistance almost always appears when the fatigue phenomena of the materials arise from the prolonged action of static and cyclic stresses.

A material subject to fatigue under the influence of the working medium may undergo either reversible or irreversible changes; here the material softens in the majority of cases; however, it is also possible for the material to harden, for example, where molten tin acts on steel under cyclic loading.

The fatigue resistance of metals is reduced (without stress concentrators) under the corrosive action of the medium. This reduction is the more vigorous the more thermodynamically unbalanced the structure of the metal; thus, reduction in the conventional fatigue strength for martensite may reach several thousand per cent as compared with the fatigue strength in air.

Media that cause erosion and cavitation damage of metal also decrease the fatigue resistance, usually as a result of irregular wear and formation of stress concentrators. Media whose radioactive decay causes exposure of structural materials to thermal neutrons give rise to an increase in the fatigue resistance with negligible time and intensity of the integral flux, while it decreases under prolonged exposure or with high irradiation densities.

There are media which dissolve structural materials; reduction in fatigue strength, which is caused basically by nonuniform solution and formation of stress concentrators, is usually observed in this case. This phenomenon is observed in certain metallic melts as regards behavior toward ferrite-based alloys. Media whose reaction with struc-

tural materials leads to formation of a chemical compound or solid solution may give rise to an increase or decrease in the fatigue resistance of the material. This depends on whether the newly forming material is stronger or weaker than the initial structural material operating under fatigue load; here, an increase in fatigue resistance is also possible in cases of formation of a weaker material when residual compressive stresses appear in the subsurface layer, as is observed, for example, when molten tin acts on steel; this was first observed in our laboratory by M.I. Chayevskiy.

A peculiar aspect of the investigations of metal fatigue resistance in working media is linked with the imposition of surface and diffusion phenomena upon the purely mechanical phenomena of fatigue. Different working media may exert a different influence on the fatigue resistances of the materials; in spite of everything, however, it is possible to isolate certain factors that are common to the majority of media and all materials and from study of which it is necessary to set up investigations in the field of the influence of the external media on fatigue resistance.

Because adsorption is observed from the majority of media and precedes the corrosion and diffusion phenomena, it is possible to speak of the universal nature of the effect of this external factor on the mechanical properties of materials. The adsorption of the medium's surface-active elements gives rise to a reduction in the level of surface energy on the solid; here deformation and failure of the solid are facilitated, since the origin of plastic shears and growth of defects are possible even under smaller stresses; this last phenomenon is known as Rebinder's effect.

Adsorption from the external medium may exert a major influence upon the mechanical properties of solids, including their fatigue re-

sistance. Reduction in the level of surface energy as a result of adsorption may even lead to spontaneous dispersion — decomposition of the metal into colloidal-size particles —, generally without applying external loads or under extremely small stresses. P.A. Rebinder and V.I. Likhtman investigated and explained these phenomena and pointed out the effect of such vigorous surface-active substances as low-melting liquid metals on the monocrystals of various metals.

Strong surface-active media usually cause softening of structural materials, while weak media, depending upon the conditions, give rise to either softening or hardening owing to plasticizing of the material, in the latter case furthering "training" of the metal, which effects an increase in fatigue resistance. Plasticizing of metal on adsorption is explained by the lowering of the energy barrier on emergence of dislocations on the free surface.

Adsorption phenomena develop both at and inside the interface of the medium and solid and in the latter case by two mechanisms: by adsorption migration from the external medium into the solid through the developed surfaces of the defects and by diffusive emergence, at the internal phase interfaces, of the surface-active elements dissolved in the solid.

The resistance of a metal to fatigue usually decreases as a result of the adsorption reaction between the external medium and the metal that is being deformed. This extremely common effect, which is caused by "adsorption fatigue" is wholly analogous to the reduction in surface tension on the given interface under the influence of adsorption, and is the more vigorous the more active the medium.

Another universal factor, which emerges with reaction between materials under cyclical loading and the external media, is linked with a property of the solids: their defective structure, the presence

- 18 -

in solids of various statistically distributed defects (from ultra-microscopic to macroscopic size). The dislocations and vacancies which predetermine the deformation of solids are also classed as defect properties.

A characteristic feature of the defective nature of solids is its development in the deformation process and concentration of these defective properties in the subsurface layers of the solid and at the interfaces between the grains and inclusions inside the solid, i.e., in zones where the solid may be in contact with the working medium. The surface tension gradient, which is linked with the surface curvature and variable surface energy density of the solid, exerts an influence on the development of surface defects at the interfaces of different phases. The adsorption from the external medium facilitates development of the defective properties.

The defective structure of the solid permits reaction between the external medium and considerable volumes of the solid with deep penetration of the external medium into the solid by two-dimensional adsorption migration through the surfaces of these defects. Plastic deformation, which facilitates development of the defects, particularly dislocations, vacancies and their coagulation, thereby contributes to the adsorption penetration of the external medium deep into the metal.

Reactions between certain types of active media and dislocations are characteristic. It is known that the dislocations and volumes of the metal near the dislocations may serve as paths for deep penetration of the external medium into the metal. The principal factor of the reaction between the external medium and the dislocations, however, is the blocking of the dislocations by the active elements of the medium, which gives rise to brittleness of the material.

The atoms of the elements dissolved in the solid solutions which form as a result of the action of the medium may obstruct the dislocations due to formation of <u>outer</u> Cottrell clouds by the familiar scheme. The formation of the <u>inner</u> Cottrell clouds, which is observed on absorption of hydrogen and also gives rise to loss of plasticity, is more interesting.

According to our presentations, the active components of hydrogen — protons — fill the dislocations and vacancies, and by transforming into the molecular state, block their movement. Accumulation of molecular hydrogen in the dislocations and vacancies with prolonged absorption of hydrogen even results in formation of hydrogen blisters and cracks, which we have observed visually.

An important factor which we must consider when studying the influence of the medium on the fatigue resistance of solids is the change in the energy level of the solid on deformation. Deformation, which increases the energy level of the solid, thereby reduces the additional activation energy needed for chemical, electrochemical diffusion and other types of reactions between the medium and solid.

The irregular action of the medium, which is linked with irregular activation of the individual portions of the metal on deformation, for example, due to uneven work hardening, residual stresses and similar phenomena that arise even before the fatigue process begins, contributes to facilitation of metal failure from fatigue. Therefore, the preliminary deformation of the metal prior to prolonged loading in active media may be found decisive in evaluating the fatigue resistance of a component in the medium.

Thus, reaction between the external media and the metal is intensified considerably in the deformation process; this refers to both the adsorption action of the external media and other types of

- 20 -

reactions. Actually, the increase in the energy level of the metal as a result of its deformation is responsible for a lower ion work function in corrosion processes, since the metal ions may vacate the lattice more readily in this case. Moreover, deformation of polycrystalline metals gives rise to internal stress gradients between the individual parts of the metal (for example, grains); in isolated regions, this irregular deformation increases the potential difference which exists between the anodic and cathodic zones, i.e., the action of the electrochemical pairs increases within the same component. The zones with the least distorted lattice (the anodic zones) are subject to corrosive attack while deposition of the hydrogen ions, which leads to hydrogen embrittlement of the metal, takes place on the cathodic zones.

In our opinion, failure from corrosion fatigue in high-stress regions develops through precisely these hydrogenized zones of the metal.

Irregular deformation (both elastic and plastic) also increases the diffusive penetration of the elements of the external medium into the solid. In this case, diffusion into the evenly deformed zones of the solid proceeds at a relatively low rate, while it takes place at a high rate through the defects that have evolved, including those of the dislocation type; in this case, we should speak of surface diffusion rather than that of the integral type.

If we consider the above factors, it is possible to explain a series of interesting phenomena observed in metal fatigue in active media. Let us dwell on the simultaneous influence of stress concentrators and active media. Since the maximum distortion of the metal lattice occurs and the first signs of plastic deformation appear in zones of stress concentration, these zones are most active in the ad-

- 21 -

sorption, electrochemical and diffusion processes. Therefore, it is possible to plasticize zones with stress concentration and reduce their negative influence on fatigue, which we observe, for example, in certain metallic melts. Another type of medium reaction is possible when vigorous local solution or corrosive attack at the bottom of the stress concentrator dulls it and effects a reduction in the concentrator's influence on fatigue resistance, which is observed in certain metallic melts and corrosive media.

The influence of surface machining on metal fatigue in active media also requires study, taking into account changes in the metal as a result of machining. The influence exerted by stress concentrators appearing as a result of machining on fatigue resistance in active media is explained above. The appearance of work hardening and residual stresses gives rise to metal activation which increases the influence of the medium on fatigue resistance in the case of irregular work hardening and residual-stress gradients in particular. In these cases, a sharp reduction in fatigue resistance occurs, for example, that which we observed in corrosive media for specimens machined by power cutting which creates two spiral strips on a surface with variable workhardening. High-speed cutting, which produces a more thermodynamically uniform surface, contributes to increased fatigue resistance in active media.

In view of the above, we should turn our attention to intensification of the influence of technological heredity, i.e., the influence of the production processes that precede finish machining, on metal fatigue resistance in active media. In cases when finish working does not put an end to thermodynamic nonhomogeneity of the subsurface layer which is produced by previous machining, the medium acts on the material selectively, giving rise to stress concentrators and reducing

fatigue resistance. Such finish-working processes as surface rolling, which suppresses all the variations caused by previous types of working, as well as creating uniform work hardening on the surface, is extremely advantageous for components operating in active media. It is necessary to remember that surface rolling and other types of uniform surface work hardening eliminate surface defects through which the medium can penetrate into the metal, thereby increasing fatigue resistance.

Manu-
script   [List of Transliterated Symbols]
Page
No.

15   ИФХ = IFKh = Institut fizicheskoy khimii = Institute of
          Physical Chemistry

15   ИМАШиА = IMAShiA = Institut mashinovedeniye [i avtomatika] =
          = Institute of Machine Construction [and Automation]

CORROSION-FATIGUE RESISTANCE OF CAST BRASS

V.A. Bykov and G.N. Vsevolodov

The technique of casting screw propellers of LAMtsZh68-5, 5-2-2 aluminum brass was developed by the Baltiysk plant in 1958 for the purpose of increasing the operating durability of medium and heavy-duty screw propellers. The above alloy possessed elevated resistance as compared with the LMtsZh55-3-1 brass usually employed for screw propellers. Metallographic investigations were conducted and the corrosion resistance and mechanical properties studied for the aluminum brass.

One of the divisions of this study was made by the Leningrad Shipbuilding Institute under contract with the plant on blanks cast by this plant. The shipbuilding institute investigated the mechanical properties and corrosion-fatigue resistance of the two screw brasses under consideration for the purpose of ascertaining advantages of one alloy over the other. The limiting states of the brasses governed by the deformation and stressing of the screw propellers and by the activity of the external medium were, as far as possible, reproduced in testing the specimens.

The results of the investigations obtained on joint study by the Leningrad Shipbuilding Institute, the Baltysk plant and other organizations are set forth below.

LIMITING STATES OF SCREW PROPELLER MATERIALS

The material of a screw propeller experiences high stress in operation as a result of water pressure on the delivering surfaces of

the blades. The pressure varies in a cyclical pattern as a function of the nearness or distance of the blades from the hull and may give rise to a certain vibration [4]. Conditions of fatigue cracking are created in cases of cyclic overstress for screw propellers operating in sea water. Cracks arise at the root sections on the delivering side of high-speed screw propeller blades [5, 6]. The danger of hydrodynamic erosion arises on cavitation [2]. In the case of short-term overloading, the plastic strength is exhausted; for example, considerable bending and breakage of the blades may occur on impact with chance obstacles.

Idle screw propellers may experience the effect of residual stresses which are particularly significant after repair of defects by welding. Residual tensile stresses give rise to the danger of corrosion cracking of brass blades with an elevated zinc content corresponding to the β structure [2].

The conditions cited above, which characterize the limiting state of the screw propeller material, were reproduced in the present investigation (with the exception of hydrodynamic erosion). The following data were taken from the test results of the specimens:

a) the ultimate stresses in various types of plastic deformation and stress rigidity are smaller, equal to or larger than those for axial tensioning;

b) the capability of plastic deformation on increasing stress rigidity and cooling;

c) the dependence of the ultimate tensile stress in corrosion cracking upon the holding time in a moist ammonia medium;

d) the dependence of the ultimate cyclic stress upon durability on bending specimens in sea water.

Investigation of Strength in Various Types of Plastic Deformation

Smooth specimens were tested in various types of deformation, to which the following stress rigidity coefficients corresponded in conformity with the strength theories (first and fourth) [1]: 0 in compression, 0.58 in torsion, 1.0 in tension, 1.0 for tension on the convex side of a bent narrow strip and 1.13 for a wide one.

Notched specimens were tested for even greater stress rigidity. Menage profile specimens 5, 10 and 20 mm thick were bend-tested. Off-center tension tests were conducted on flat specimens with a notch on the elongated side and a section of 70 x 17 mm at the notch; these specimens were tested both at room temperature and on cooling to the temperature of liquid nitrogen.

Good convergence of the ultimate stresses in tension, compression and torsion was found for the smooth specimens; the yield points converged under torsional stresses in accordance with the fourth theory

TABLE 1

Chemical Composition and Mechanical Properties of Cast Brasses

1 Латунь	2 Химический состав, вес. %	σ_T,	σ_b,	S_k,	ψ, %	δ, %
		3 кг/мм²				
4 ЛМцЖ55-3-1	Cu — 54,61; Mn — 3,31 Fe — 0,81; Zn — 40,97	20	54	76	30	30
5 ЛАМцЖ68-5, 5-2,2	Cu — 68,28; Mn — 2,69 Fe — 2,12; Zn — 21,44; Al — 5,45	30	64	83	22	25

1) Brass; 2) chemical composition, % by weight; 3) kg/mm²; 4) LMtsZh55-3-1; 5) LAMtsZh68-5, 5-2,2.

and the breaking strength decreased for torsional stresses in accordance with the third theory. The brass specimens deformed almost uniformly over their length up to failure. The ability to concentrate

strain was not detected. Therefore, the cast brass specimens were brought to failure even in compression.

Table 1 lists the chemical compositions of the brasses and the data from tension tests of the smooth specimens, which are indicative of fundamental mechanical properties.

The following was established as a result of testing specimens that were more rigidly stressed than those in axial tension:

1. Smaller bending angles and residual fiber stresses were observed on wide blades than on narrow blades as a result of biaxial stressing where the thickness of both blades was the same. In both types of specimens, however, significant plastic deformation and considerable energy absorption preceded failure.

2. Increased width of the notched Menage specimens led to a certain reduction in ultimate plasticity, but without transition to brittleness.

3. Even extremely vigorous cooling did not effect a reduction in the plasticity of the brasses before rupture or in the ultimate load in off-center tensioning of flat notched specimens.
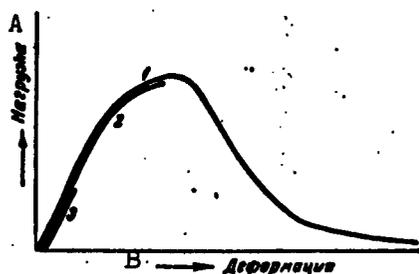
Fig. 1. Curves of deformation resistance (schematic). 1) Viscous state; 2) limited viscous state; 3) brittle state. A) Load; B) deformation.

We may assert on the basis of the experimental data that under any unfavorable conditions, plastic deformation precedes the failure of the cast brasses investigated. As compared with the brittle state, an essential redistribution of stresses, which always guarantees a high ultimate load prior to failure of the brasses (Fig. 1, curve 1), occurs as a result of this deformation. It is this that favorably distinguishes brass from many structural

- 27 -

steels, which lose their ability to deform plastically under unfavorable conditions (curves 2 and 3), and may fail under negligible ultimate load [1].

Investigation of Corrosion-Mechanical Resistance

Resistance to corrosion cracking was investigated on smooth specimens placed in a vessel over a 25% aqueous solution of ammonia.

The investigation was conducted by two methods: 1) the specimens were slowly elongated over several hours to rupture; the test was accompanied by the formation of fine transverse cracks under the action of the tensile stresses and the corrosive medium; this led to a reduction in strength and ultimate plasticity; this reduction appeared in an extremely acute form in LMtsZh55-3-1 brass and was negligible in LAMtsZh68-5, 5-2-2 brass; 2) elongated or curved prestressed specimens were tested, showing that LMtsZh55-3-1 brass cracked under much lower stresses and in less time than did LAMtsZh68-5, 5-2-2 brass.

Flat specimens 15 x 25 mm in section were tested for endurance over a prismatic-section length of 100 mm. As a result of forced deformation, the specimens were subject to pure bending in a symmetrical cycle at a frequency of approximately 500 cycles/min. The specimen sections being deformed were enclosed by a rubber casing filled with artificial sea water (the volume reached $100.\ cm^3$). The salt content per 10 liters of water was NaCl — 265.18 g, anhydrous $MgSO_4$ — 33.05 g, CaCl [sic] — 11.4 g, hydrated $MgCl_2$ — 24.47 g, KCl — 7.25 g, NaBr — 0.83 g and $NaHCO_3$ — 2.08 g. The water was changed daily in checking specimen stressing. Bending stresses were established in accordance with the proportionality law from measurements of the longitudinal fiber strain. The latter was measured with a lever-switch-and-indicator-type straingauge (base 20 mm) with a magnification of 1000 times.
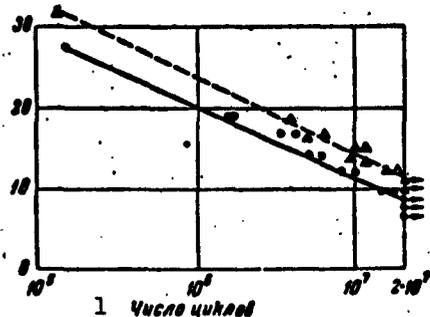
Fig. 2. Corrosion resistance curves of cast brasses in symmetrical-cycle bending.
▲ — brass with aluminum, N_t;
● — same, without aluminum;
△ — brass with aluminum, N_v;
○ — same, without aluminum.
1) Number of cycles.

A series of 7-9 specimens of each brass was examined. Cyclic lives of 10^5 to $2 \cdot 10^7$ cycles corresponded to different ultimate stresses.

The durability corresponding to the ultimate stress of each specimen was determined from the appearance of metal fatigue weakening as indicated by the sharp increase in the readings of the device used to measure the amplitude of specimen fiber deformation (N_T) and the fatigue cracks (N_v) visible to the naked eye. These two durability values differed markedly, particularly under small ultimate stresses. The formation of sets of fatigue cracks with one main crack occurred as the tests progressed; this is characteristic for corrosive conditions. The results of the endurance tests are shown in Table 2. The endurance curve of LAMtsZh68-5, 5-2-2 aluminum brass was found to lie above that of LMtsZh55-3-1 brass (Fig. 2). At a durability of $2 \cdot 10^7$ cycles, the endurance limit for LAMtsZh68-5, 5-2-2 was 11.5 kg/mm^2 and 9 kg/mm^2 for LMtsZh55-3-1. These endurance limits were found to be considerably lower than the strength characteristics of these same brasses in plastic tension (see data c: Table 1).

In view of this, the question arises as to which of the above ultimate stresses may be the fundamental allowable stress for the design of new screw propellers. According to V.M. Lavrent'ev [3], an allowable stress [σ] in the range from 400 to 800 kg/cm^2 is recommended for screw propellers of manganese brass. This value approaches the endurance limit of brass, but is considerably smaller than σ_t

- 29 -

or σ_b. Therefore, we may assume that the real ultimate stress of the screw propeller material is close to the limit of corrosion endurance. This same supposition evidently directed the attention of foreign investigators to study of the corrosion endurance limit of screw-propeller materials [5, 6].

TABLE 2

Results of Corrosion Endurance Tests on Flat Specimens

3 № образца	1 ЛМцЖ55-3-1			2 ЛАМцЖ68-5,5-2-2		
	4 σ, кз/мм²	5 N_T, тыс. циклов	6 $N_в$, тыс. циклов	4 σ, кз/мм²	5 N_T, тыс. циклов	6 $N_в$, тыс. циклов
1	27,6	152	152	32,1	131	131
2	18,9	1 500	1 630	18,9	3 974	3 974
3	16,5	3 300	4 100	16,7	4 900	6 530
4	13,9	4 900	5 900	15,1	9 966	11 972
5	12,x	8 300	10 100	14,1	9 830	12 218
6	9,6	14 490	18 104	12,5	15 800	19 070
7	8,7	>20 000	>20 000	11,6	>20 000	>20 000
8	7,8	>20 000	>20 000	10,3	>20 000	>20 000
9	6,7	>20 000	>20 000			

1) LMtsZh55-3-1; 2) LAMtsZh68-5, 5-2-2; 3) specimen No.; 4) σ, kg/mm^2; 5) N_T, thousands of cycles; 6) N_v, thousands of cycles.

CONCLUSIONS

The ultimate stresses, which characterize the strength of cast brass — a screw-propeller material — were studied in the paper. These stresses were obtained from tests which reproduced the operating conditions of screw propellers (with the exception of hydrodynamic erosion) on the specimen.

The ultimate stresses of LAMtsZh68-5, 5-2-2 brass were found to be greater than those of LMtsZh55-3-1 brass. Neither brass manifested tendencies to brittle failure under rigid stressing conditions.

In view of the alternating stressing of blades of screw propellers operating in sea water, corrosion endurance tests were conducted on specimens in two-dimensional cyclic bending with a sym-

metrical cycle. For endurances to $2 \cdot 10^7$ cycles, the ultimate stresses of LAMtsZh58-5, 5-2-2 brass were found to be higher than those of LMtsZh55-3-1 brass.

Of the ultimate stresses studied for screw-propeller brasses, the limits of corrosion endurance approximate most closely the stress allowable for strength calculations for the propellers.

REFERENCES

1. V.A. Bykov, Plastichnost' i prochnost' konstruktsionnoy stali. Sudpromgiz [Plasticity and Strength of Structural Steel. State Publishing House for the Shipbuilding Industry], 1959.

2. I.N. Voskresenskiy, Korroziya i eroziya sudovykh grebnykh vintov [Corrosion and Erosion of Ship Screw Propellers], Sudpromgiz [State Publishing House for the Shipbuilding Industry], 1949.

3. V.M. Lavrent'yev, Sudovyye dvizhiteli [Marine Movers], Izd-vo Morskoy transport [State Publishing House for Literature on Maritime Transport], 1949.

4. N.Ya. Stel'makh, Elektrotenzometricheskiye issledovaniye deformatsiy v lopastyakh sudovogo grebnogo vinta. Trudy LIIVT [Electrotensometric Investigation of Deformations in Blades of Ship Screw Propellers. Trans. of the Leningrad Institute of Water Transport Engineers], No. 23, 1956.

5. F. Hudson, The Development of High Tensile Aluminum Bronze. Alloys for Marine Propellers in Great Britain, USA. The Shipbuilder and Marine Engine Builder, XII, N-12, 1957.

6. Lee Williams, Aluminum Bronzes for Marine Applications. J. of the American Society of Naval Engineers [Inc.], Aug. 1957.

Manu-script Page No.	[List of Transliterated Symbols]
29	T = T = tenzometr = straingauge
29	в = v = vidimyy = visible
29	т = t = tekuchest' = yield, flow

INFLUENCE OF LOW-MELTING METALLIC MELTS ON FATIGUE RESISTANCE OF CARBON AND CHROMIUM-NICKEL STEELS

M.I. Chayevskiy

Molten metals are employed as heat carriers in a number of machines and apparatus. During operation, the components of these machines and apparatus may be subjected to stresses which vary cyclically and arise on periodic change in both the force load and the temperature. Therefore, proper attention should be given to investigation of the influence of metallic melts on the fatigue resistance of steels.

The influence of low-melting metallic melts on the mechanical properties of steels is associated with different types of physico-chemical effects (adsorption and diffusion processes and chemical reactions). It is known that the fatigue resistance of steel may diminish considerably as a result of the adsorption effect of a surface-active medium [1]. There are examples, however, in which the medium does not exert a harmful influence on the resistance of solids or even increases it. Thus, a significant increase in the fatigue resistance of steel specimens with stress concentrators exposed to an Sn or Pb + Sn eutectic melt was detected in References [2, 4]. This increase in resistance was explained earlier by plasticizing of the bottom of the concentrator by the melt, with the result that stress concentration is reduced.

In view of the above positive influence of tin or lead-tin melts on steel under cyclical deformation, it would also be interesting to

study whether other melts result in a similar effect. The experiments that have been conducted give a negative answer. As is seen from Figs. 1-3, a sharp drop in the fatigue resistance of steel specimens with stress concentrators is observed with the action of the Pb + Bi eutectic melt. Consequently, the effect of increased fatigue resistance with the action of a tin or Pb + Sn-eutectic melt results not only from plasticizing, but also from those diffusion and chemical processes which take place on contact between deformed steel and tin.

In order to confirm this supposition, fatigue resistance tests in the Pb + Sn eutectic melt were undertaken by a method somewhat different from that used earlier [2-4]. Specimens plated with the Pb + Sn eutectic were tested in air at the same temperature at which they were previously tested for fatigue resistance in a pool with the Pb + Sn eutectic melt. As is seen from Fig. 1 (curve 1) and Fig. 3 (curve 7), the durability of the specimens remained high in the process. It is essential in these experiments that the surface film of the melt undergoes oxidation during the tests and consequently, the plasticizing effect will disappear. Nevertheless, the specimen continues to endure increased cyclic loading [5].

On the basis of this, we might assume that plasticizing of steel by the melt does not exert an influence on the effect of increased fatigue resistance, and that it is entirely a matter of the physico-chemical processes that arise on tinplating of steel. Experiments do not confirm such an inference, because tin-plated specimens that are tested at room temperature have fatigue resistance limits lower than specimens that are not plated with tin (see Fig. 3).

Attention is also drawn to experiments that directly indicate the major role of steel plasticizing by the melt at the start of cyclic
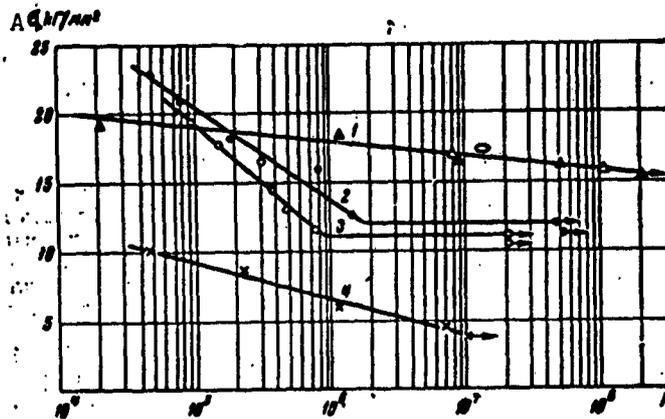
Fig. 1. Fatigue resistance curves of
specimens with stress concentrators (nor-
malized steel 50, frequency of stress
variation n = 50 cycles/sec). 1) Tests
of specimens plated with Pb + Sn eutec-
tic in air at 400° (control points ob-
tained on testing tin-plated specimens
in cup with Pb + Sn eutectic melt are
keyed by open triangles); 2) tests in
air at 400°; 3) same, at 20°; 4) tests
of tin-plated specimens in Pb + Bi eu-
tectic melt at 400°. A) σ, kg/mm^2.

deformation. As we know [6], fatigue resistance tests of previously

unplated specimens conducted in a lead-tin melt may lead to signifi-

cant reduction in fatigue resistance. Consequently, only the joint

influence of the plasticizing effect and other physicochemical pro-

cesses at the start of cyclic deformation may lead to an increase in

the fatigue resistance of steel.

The plasticizing effect is the most general, universal effect of

a surface-active medium, and one which always arises on deformation

of metal in any surface-active medium [7]. It is associated with

facilitation of dislocation outcropping on the surface of a deformed

metal. Moreover, the major role in the plasticizing effect may belong

to superficial (having one point of attachment) dislocation sources

whose initial operating stress is considerably lower than that of

- 34 -
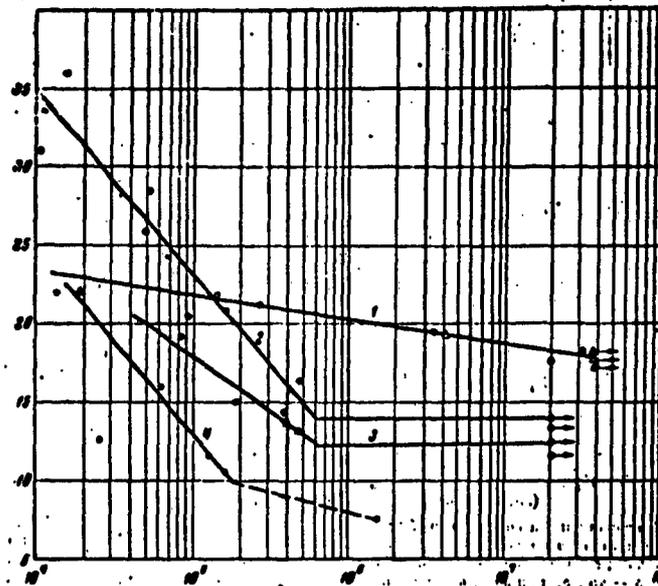
Fig. 2. Fatigue resistance curves of speci-
mens with stress concentrators (thermally
improved steel 50, quenching in water from
$850°$, tempering at $590°$, n = 50 cycles/sec).
1) Test of specimens previously plated with
Pb + Sn eutectic, in Pb + Sn eutectic melt
at $300°$ (control experiments where tin-
plated specimens were tested in air are keyed
by triangles); 2) tests in air at $20°$; 3)
same, at $300°$; 4) tests of tin-plated speci-
mens in Pb + Bi eutectic melt at $300°$. A)
σ, kg/mm^2.

sources with two-point attachment. Reduction in surface energy should

lead to increased activity of the subsurface sources and to a decrease

in the yield point of the material [8]. Consequently, the essential

nature of the positive influence of surface layer plasticizing of

metal at the start of cyclic deformation consists in relief of the

local internal normal stresses that arise at accumulations of disloc-

cations on the surface layer of metal, which may be a major obstacle

for dislocations that move in the normal state [9].

We should remember, however, that the effect of plasticizing can

lead to an increase in fatigue resistance only in cases when some obstacles impede continuous penetration of the melt into the metal through evolving defects. No such obstacles form when the Pb + Sn eutectic melt acts upon steel under cycle deformation; therefore, a significant drop in fatigue resistance occurs. In the given case, we are essentially concerned only with the effect of the adsorption decrease in cyclic endurance, since neither lead nor bismuth reacts chemically with steel at the temperatures used in the tests [10]. We should note that a similar phenomenon of sharp decrease in the fatigue resistance of steel under the action of mercury was detected earlier in study [11].

The process takes place otherwise with steel under cyclic deformation in a tin or Pb + Sn eutectic melt. Diffusing into the interior of the metal through evolving defects, the tin melt enters into chemical reaction with the steel, forming an $FeSn_2$-type intermetallic compound. The cell size of the $FeSn_2$ lattice is larger than that in the Fe lattice; therefore, compressive stresses, which impede penetration of the tin melt into the interior of the metal, arise in the surface layer of the metal. Naturally, tin from the melt will also penetrate by diffusion through the intermetallic layer into the interior of the metal. When Fe is encountered, however, chemical reaction will again take place, forming new compact volumes of metal. This is why solution of the surface layers of steel does not result in removal of compressive stresses in tests in a pool with a tin or Pb + Sn eutectic melt.

As was indicated in Reference [12], compressive stresses forming in carbon steel are stable in a rather wide temperature range.

Experiments conducted with smooth specimens made of hardened steel 50 and with specimens having stress concentrators led, at first

- 36 -
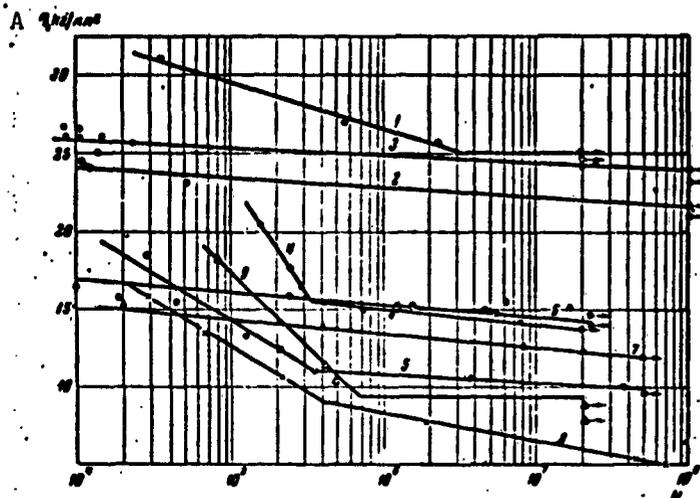
Fig. 3. Fatigue-resistance curves of 1Kh18N9T steel specimens (quenching in water from 1150°, n = 40 cycles/sec). 1) Tests in air at 20°; 2) same, at 500°; 3) test of specimens previously coated with Pb + Sn eutectic melt, in Pb + Sn eutectic melt at 500°; 4) test of specimens with stress concentrators in air at 20°; 5) same, at 500°; 6) test of specimens with stress concentrators plated with Pb + Sn eutectic, in melt of Pb + Sn eutectic at 500° (tin plating at 400° using ammonium chloride as flux); 7) test of specimens plated with Pb + Sn eutectic, in air at 500°; 8) test of specimens plated with Pb + Bi eutectic, in melt of Pb + Bi eutectic at 500°; 9) test of specimens plated with Pb + Sn eutectic, at 20°. A) σ, kg/mm².

glance, to contradictory results. As we see from Fig. 4, the fatigue resistance of the smooth specimens diminishes under the action of the Pb + Sn eutectic melt by approximately 47% as compared with tests in air. At the same time, the fatigue resistance of the specimens with stress concentrators not only uid not decrease under the action of the Pb + Sn eutectic melt, but even increased somewhat. It is necessary to assume that a certain increase in the fatigue resistance of specimens with stress concentrators under the action of a metallic melt as compared with tests in air is an effect of the above-described mechanism of surface-layer hardening as a result of the formation of

- 37 -

an intermetallic compound.

The cause of the drop in the fatigue resistance of smooth hardened specimens that are exposed to a metallic melt should be sought in microfailures of the steel that originated in the hardening process. The point is that macro- and microcracks [13], which reduce fatigue resistance on testing in air, may form in steel specimens on rapid quenching (in water). In cases of the melt falling into these cracks, the latter begin to develop so rapidly that chemical reaction with the formation of the intermetallic compound cannot take place and we observe an adsorption decrease in fatigue resistance.

We should emphasize that in order to ascertain the effect of increased fatigue resistance under the action of the Sn or Pb + Sn-eutectic melt, it is necessary that the diffusion process and the chemical reaction between the tin and iron take place more rapidly than formation of the defects and microcracks. Otherwise, the durability of the specimens on testing in the Sn or Pb + Sn eutectic melt will diminish as compared with testing in air. As we see from Figs. 1-4, the limited endurance of specimens that are tested in a melt under considerable stresses is less than that on testing in air (see also [2-4]). This also explains the fact that a sharp drop in ultimate strength is detected (at certain temperatures) under the action of the tin or Pb + Sn eutectic melt (Fig. 5) in tension tests of specimens with stress concentrators, although the fatigue resistance increases (see Figs. 1 and 2) at the same temperatures and under the action of the same melts.

It is not yet possible to conclude the inapplicability of hardened components for operation in metallic melts on the basis of the drop in the fatigue resistance of smooth hardened specimens that was detected by experiment. It is found that if we begin the tests with

- 38 -
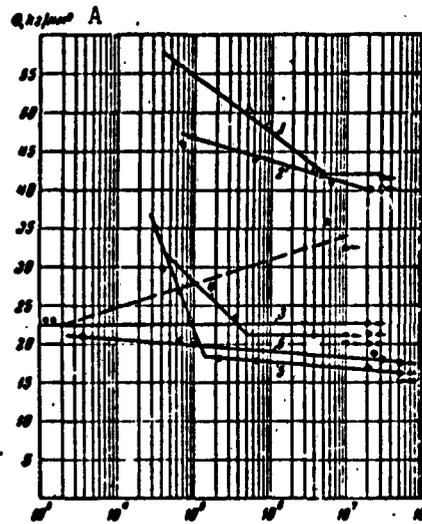
Fig. 4. Fatigue resistance
curves of hardened steel 50
specimens (quenched in water
from 850°, n = 50 cycles/sec).
1) Test of smooth specimens in
air at 20°; 2) same, at 300°;
3) test of smooth specimens
plated with Pb + Sn eutectic,
in melt of Pb + Sn eutectic
at 300°; 4) test of specimens
with stress concentrators in
air at 20°; 5) same, at 300°;
6) test of specimens plated
with Pb + Sn eutectic, with
stress concentrators in melt
of Pb + Sn eutectic at 300°.
A) σ, kg/mm^2.

Fig. 5. $\sigma = f(\varepsilon)$ curves for
normalized steel 45 speci-
mens with stress concentra-
tors. 1, 2, 3, 4, 5, and 6)
Tests in air at temperatures
of 300, 400, 500, 550, 600
and 650°, respectively. I,
II, III, IV, V and VI) Tests
of specimens plated with
Pb + Sn eutectic, in Pb + Sn
eutectic melt at tempera-
tures of 300, 400, 500,
550, 600 and 650°, respec-
tively. A) σ, kg/mm^2.

stresses from 21-22 kg/mm^2 and increase them gradually (in our ex-
periments, after every 10^7 cycles), the load withstood by the speci-
mens may increase considerably. The corresponding points are keyed
by triangles in Fig. 4.

We should note that the conclusion [14] that the effects of
stress concentration and medium are not additive was drawn on in-
vestigation of the simultaneous influence of medium and stress con-
centrators on fatigue resistance; the effects do not aggravate one
another but, conversely, both factors in joint action show decreased

Fig. 6. Microsection of thermally improved
steel 50 specimen tested in Pb + Sn eutec-
tic melt at 300°, $\sigma = 19.6$ kg/mm^2, $N = 2 \cdot 10^7$ cycles, 200x.

influence on fatigue resistance. This is because the corrosive medium
itself creates a large number of concentrators in the form of corro-
sion cracks; but since addition of supplementary concentrators to the
base may exert an unloading influence on the fundamental concentrator,
this results in decline of the influence of the concentrator on
fatigue strength in a corrosive medium.

The majority of molten metals dissolve steel at elevated tempera-
tures. However, as is apparent from Fig. 6, the most vigorous solu-
tion of steel and intrusion of the melt into cracks develop in the
direction of maximum normal stresses. In the given case, therefore,
it is impossible to speak of a reduction in stress concentration as
a result of solution.

An approximate determination of the magnitude of the compressive
stresses that arise in the surface layer of steel as a result of forma-
tion of an intermetallic compound may be established by using the
method of ring sections, which was proposed by N.N. Davidenkov [15].

Figure 7 shows the nature of the stress variation in the inter-

metallic surface layer of a split ring on heating to 400°. As we see, on heating the ring to 400°, the small residual tensile stresses present at room temperature are converted into significant compressive stresses which are the cause of increased fatigue resistance.
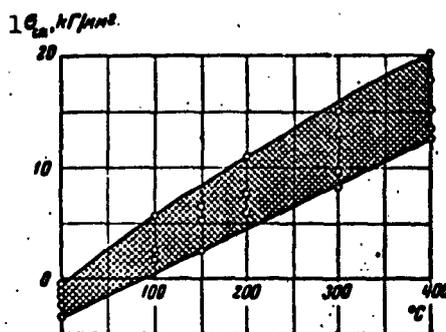
Fig. 7. Nature of residual stress distribution in intermetallic surface layer of split ring on heating to 400°. Cup from which ring was cut was exposed to tin melt at 400° for 73 hours. 1) σ_{szh}, kg/mm^2.

On the basis of the above, we may draw the following conclusions:

1. The fatigue resistance of steel may increase under the action of a low-melting metallic melt.

2. This increase occurs only in cases where an intermetallic layer and residual compressive stresses form in the surface layer of steel as a result of adsorption, diffusion and chemical processes (at the outset of cyclic deformation).

3. A decrease in the fatigue resistance of steels takes place in cases of only adsorptive activity of the melt.

Manu-
script   [List of Transliterated Symbols]
Page
No.

41   cx = szh = szhimayushchiy = compressive

REFERENCES

1. V.I. Likhtman, P.A. Rebinder, and G.V. Karpenko, Vliyaniye pover-khnostno-aktivnoy sredy na protsessy deformatsii metallov. Izd-vo AN SSSR [Effect of Surface-Active Medium on Deformation Processes of Metals. Publishing House of Acad. Sci. USSR], 1954.

2. M.I. Chayevskiy, Sb. Deyaki pitaniya fiziko-khimichnoi mekhaniki metaliv, Izd-vo AN USSR [Certain Problems of the Physicochemical Mechanics of Metals. Publishing House of Acad. Sci. UkrSSR], 1958.

3. M.I. Chayevskiy, Dokl. AN SSSR [Proc. of the Acad. Sci. USSR], Vol. 124, No. 5, 1959.

4. M.I. Chayevskiy, Dokl. AN SSSR, Vol. 125, No. 2, 1959.

5. M.I. Chayevskiy, Avt. svid. [Author's Certificate] No. 125993, class 48v, 5/48v, 7.

6. M.I. Chayevskiy, Metallovedeniye i termicheskaya obrabotka [Physical Metallurgy and Heat Treatment], No. 8, 1959.

7. V.A. Labzin and V.I. Likhtman, Doklad AN SSSR [Proc. of Acad. Sci. USSR], Vol. 129, No. 3, 1959.

8. V.I. Likhtman and Ye.D. Shchukin, Usp. fiz. nauk [Progress in the Physical Sciences], 66, 213, 1958.

9. C.S. Barrett, Acta Metall. 12, 1953.

10. M. Hansen, Constitution of Binary Alloys, 1958.

11. G.V. Karpenko, Prikladnaya mekhanika [Applied Mechanics], 3, 1957.

12. M.I. Chayevskiy, Fizika metallov i metallovedeniye [Physics of

Metals and Metallography], Vol. 8, No. 5, 1959.

13. Ye. I. Malinkina, Obrazovaniye treshchin pri termicheskoy obrabotke stali [Formation of Cracks in Heat Treatment of Steel], Metallurgizdat [State Publishing House for Literature on Metallurgy], 1958.

14. G. V. Karpenko and F. P. Yanchishin, Dopovidi AN URSR [Proc. Ukrainian Acad. Sci.], No. 6, 1955.

15. N. N. Davidenkov, ZhTF [Journal of Technical Physics], Vol. 1, No. 1, 1931.

APPARATUS FOR STUDY OF METAL CORROSION FATIGUE

S.A. Gladyrevskaya, L.V. Ignatyuk and V.A. Svetlitskiy

Up to the present time, the cause of metal fatigue cannot be regarded as definitely established. Moreover, none of the existing schemes of the corrosion-fatigue mechanism can account for all of the phenomena that occur when steel is placed under a live load in a corrosive medium.

Determination of the moment of fatigue cracking and its post-development observation up to failure of the specimen may hold major interest for ascertaining the mechanism of the fatigue failure and the influence of the medium on the mechanism. Fixation of the initial stages of failure is always complex and modern methods of detecting cracks are rather imperfect as yet.

The effect of the frequency of stress variation on metal fatigue failure, together with other factors that influence corrosion fatigue, is extremely interesting. It is known that the process of metal fatigue is accompanied by complex phenomena of hardening and recovery, as well as the phenomena of stress redistribution among the individual grains of the metal, which take place in secondary deformation. Hardening occurs under the influence of microplastic deformations that give rise to internal interfaces in individual grains with distortion of the crystal lattice and a change in the nature of the atomic bonds [1].

The softening process is a secondary process; it is counter to the hardening process and results in loss of the internal interfaces
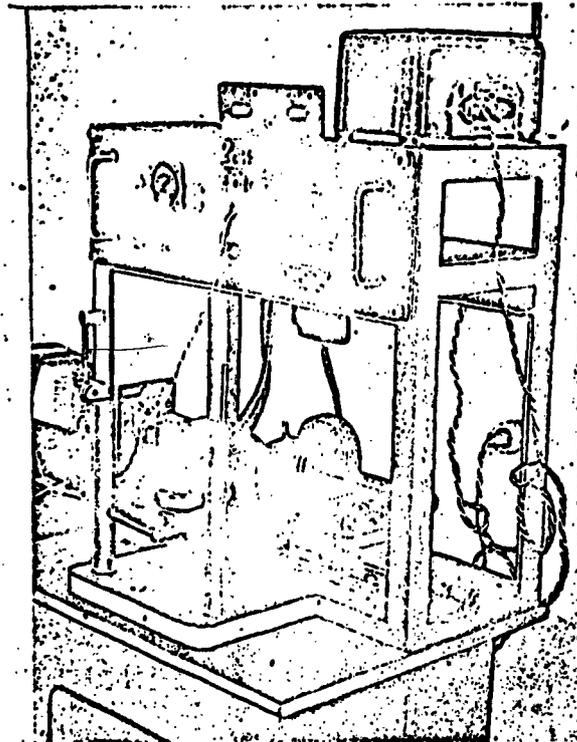
Fig. 1. General appearance of apparatus.

and distortion of the crystal lattice, as well as closing of the ultramicrocracks that open on the grain surface. Surface-active substances facilitate and considerably accelerate the plastic deformation process by penetrating into the microcrack openings [2].

The frequency of stress variation in corrosive media influences the fatigue resistance of steel, effecting a reduction in the endurance of steel with decreasing frequency, because at high frequencies an aggressive medium cannot penetrate into the microcracks opening under the influence of tensile stresses, while those microcracks that emerge with tensile stresses begin to close on the shift to compressive stress and are made inaccessible to the influence of the medium [3]. Contradictory opinions are also encountered in the

literature [4].

There are very few studies on the corrosion-fatigue resistance of metal in a low-frequency region, although many designs and mechanisms operate and fail in these frequency bands (5-30 cps).

An electromagnetic low-frequency machine that permits recording of the appearance of a fatigue crack in a specimen (Fig. 1) was designed and fabricated (at the Railroad Transportation Institute, with participation of staff members of the Department of Strength of Materials of the MVTU imeni Bauman) in a program to build new apparatus for study of the corrosion fatigue process of metals.

The apparatus consists of a mechanical part, an electronic generator and a measuring system which provides for periodic measurements of the total vibration period of the specimen — the reciprocal of its frequency.

Mechanical Part of Apparatus

The mechanical part of the apparatus, which operates on the principle of a self-oscillating system with the specimen to be tested placed in a bath with an aggressive solution (where the recovery force of the specimen and the mass of the weights determine the natural vibration frequency of the system, and therefore that of the specimen being tested), enables us to judge the specimen's fatigue and other endurance characteristics from the variation in its vibration period.

The apparatus is intended for corrosion resistance tests of flat specimens from 2 to 10 mm thick, 30 mm in width and 100 mm in effective length with loading for pure bending in accordance with the scheme shown in Fig. 2. The mechanism of the apparatus provides for stresses constant along the effective length of the specimens that are being tested.

The specimen 1 is secured in the fixed lower grip 2 and in the

- 44 -
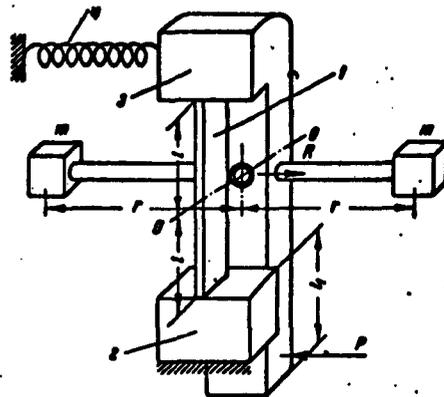
Fig. 2. Diagram of mechanical part.

movable upper grip 3. The movable grip may rotate about the O-O axis under the action of the force P (attraction of the magnet). The pivot axis of this grip runs through the center of the specimen with the result that the reaction R is equal to the force P with the condition that the rigidity of the grip is incommensurably higher than that of the specimen. The specimen will be under conditions of pure bending with the moment

$$M_1 = P(l + l_1). \qquad (1)$$

In vibration, the specimen will be loaded additionally with the moment M_2

$$M_2 = 2rF, \qquad (2)$$

where F is the inertia of the mass m.

The natural frequency of the system depends upon the rigidity of the specimen and the moments of inertia of the mass m and the grip 3. Varying the position of the mass m, we may vary the vibration frequency of the system, thereby determining the relationship of endurance limit to vibration frequency. The specimen is loaded by the spring 4 in order to obtain an asymmetrical stress cycle. The spring tension that is required to produce a specific asymmetrical cycle is established from the amount of spring elongation.

The value of the attraction P of the magnet (approximate value) may be determined from a preset stress amplitude in static work (when F = 0). In this case,

$$M_1 = \sigma_a w; \qquad (3)$$

- 45 -

where σ_v is the stress amplitude and ω is the moment of inertia of the most rigid specimen.

From Expression (1) we obtain

$$P_j = \frac{\sigma_o \omega^2}{1 + t_1}$$ (4)

Knowing the force P, we may determine the number of ampere-turns (as a function of the gap $\underline{a}$ between the armature and the poles of the magnet):

$$\omega l = \frac{\Phi_{aaz} 2a}{\mu S},$$ (5)

where F_{zaz} is the magnetic flux in the gap, μ is the magnetic permeability of air and S is the cross-sectional area of the magnetic circuit.

For more detailed study of the possible modes of operating the apparatus, let us derive the equation of motion of the armature.

The gap between the armature and magnet varies on vibration, thereby varying the force of attraction P. The force P for an arbitrary position of the armature is determined by the expression

$$P = \frac{kI^2}{(a - x)^2},$$ (6)

where $\underline{k}$ is a constant coefficient, I is the current which is dependent upon time (it is assumed that the back effect of the armature's movement on the current may be disregarded) and $\underline{x}$ is the displacement of the armature.

Expressing the system's equations of motion in terms of the linear displacement of the armature, we obtain the following equation:

$$x'' + \frac{(c_1 + c_2)l^2}{I_1} x = \frac{P(l + l_1)l}{I_1},$$ (7)

where I_1 is the moment of inertia of the grip 3 and masses $\underline{m}$ and c_1 and c_2 are the rigidities of the spring and specimen.

For small vibrations, we may assume

$$\frac{1}{(a-s)^2} \approx \frac{1}{a^2}\left(1 + 2\frac{s}{a}\right). \tag{8}$$

In this case, the equation of motion (7) takes the form

$$z'' + \left[\frac{c_1 + c_3}{I_1} - \frac{(l+l_1)\,l2k\,l^2}{I_1 c^3}\right]z = \frac{(l+l_1)\,lk\,l^2}{I_1 c^3}. \tag{9}$$

Since I is a periodic function of time, investigation of the armature movement or, what is the same thing, the vibration of the specimen, reduces to investigation of a Mathieu equation with a [nonzero] right member.

If the frequency of variation of the current I is independent of the system's vibration, investigation of Equation (9) reduces, in this case, to determination of the relationship between the parameters of the system for which a stable vibration regime will develop. In the present apparatus, it is possible to excite vibrations by using feedback. In this case, the frequency of the alternating current agrees with the vibration frequency of the mechanical part of the apparatus.

This case leads to investigation of a system of two equations (in x and I).

Exciting Generator

A tuning-fork type electronic generator, the block diagram of which is shown in Fig. 3, where O is a metal specimen, P1 and P2 are weights that determine the inert mass of the vibrating system, D is an inductive sensor, φ is a phase inverter, UN is a voltage amplifier, UM is a power amplifier, EM1 and EM2 are exciting electromagnets and Ya is an armature, is employed in the apparatus to maintain the vibrations of the mechanical system at its resonant frequency.

The vibration period of the given generator may be expressed as

$$T = 2\pi \frac{m}{\sqrt{c^2 - \frac{1}{4}a^2}}, \tag{10}$$

where m is the mass of the system, $c = F/l$ and $\alpha = R/v$, i.e., are proportionality coefficients characterizing the magnitude of the re-

- 47 -

covery force F of the specimen and the resisting force R, respectively, which are computed per unit displacement $\underline{l}$ of the specimen and per unit velocity $\underline{v}$ of its displacement.
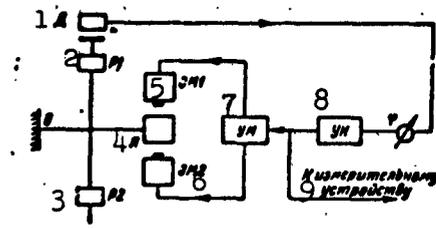
Fig. 3. Block diagram of exciting generator. 1) D; 2) P1; 3) P2; 4) Ya; 5) EM1; 6) EM2; 7) UM; 8) UN; 9) to measuring unit.
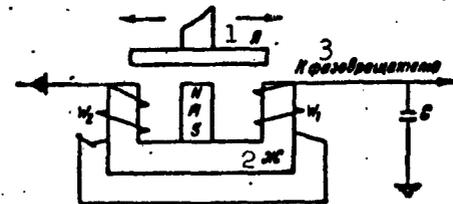
Fig. 4. Circuitry of inductive sensor. 1) Ya; 2) Zh; 3) to phase inverter.

The quantities F and R are subject to variation in the process of testing the specimens; this effects a variation in the vibration period of the mechanical system. The latter is fixed by a measurement-signaling unit.

Operation of the generator is based on the presence of a positive feedback through the vibrating part of the mechanical system with parameters Q and $R_s + R_o$.

The feedback in the generator is accomplished by the inductive sensor shown in Fig. 4 where Ya is the armature of the sensor, M is a permanent magnet, Zh is a Π-shaped iron transformer core, W_1 and W_2 are sensor coils and C is a capacitor for shifting the resonant frequency of the sensor coils into the operating-frequency region.

In the general case, the voltage that is picked off the sensor is not in phase with the exciting force of the field electromagnets without use of special measures; this may result in small specimen vibration amplitudes or in complete collapse of the generator regime. To prevent this, a phase inverter, which serves as a selsyn, is mounted at the input of the voltage amplifier.

The four-stage voltage amplifier is embraced by a selective

negative feedback for the purpose of collapsing the high-frequency region of the amplifier's frequency characteristics. The final stage of the voltage amplifier is a phase inverter for the input to the push-pull power amplifier.

The operating conditions of the voltage amplifier are selected with bilateral limitation of the output signal, in view of which a square-wave driving voltage is supplied at the tube grids of the power amplifier.

The power amplifier is built around two 6N5S tubes whose operating conditions $(R_1; R_2)$ are selected in the vicinity of the Class A mode for the purpose of creating a constant magnetic field in the gaps between the armature and the field electromagnets. The oscillating component of the current that feeds the field electromagnets is Π-shaped.

A milliammeter is incorporated into the common cathode circuit of the tubes in order to monitor the current in the arms of the power amplifier, while pushbuttons are introduced into the cathode circuits of the arms.

When there is no need to measure the current, the millisecond counter is short-circuited by a toggle switch for the purpose of preventing prolonged jolting of the counter's casing.

The gaps between the field electromagnets and armature may be varied with the micrometer screws that move the electromagnets in order to regulate the vibration amplitude of the specimen.

A pulse counter used to count the number of specimen vibrations is incorporated between the tube plates of the power amplifier via a diode. A pair of contacts, which close after every 10,000 pulses is introduced into the 10^4-capacity counter; this makes it possible to incorporate a second counter to produce a count capacity of 10^8.

- 49 -

Measuring-Signaling Unit

The fundamental problem in testing specimens is to obtain the
time dependence of the variation in the specimen's vibration period
(with the rest of the parameters constant), i.e., to obtain the re-
lationship $T = f(t)$, the diagram of which takes the form shown in
Fig. 5.

Fig. 5. Diagram of re-
lationship $T = f(t)$.
1) Frequency variation
in cps; 2) number of
cycles.

Fig. 6. Block diagram of measur-
ing-signaling unit. 1) UO; 2) BT;
3) RS; 4) SZ; 5) R1; 6) R2; 7)
R3; 8) R4; 9) U1; 10) U2; 11) U3;
12) U4.

Naturally, we may judge both the corrosion resistance and mechani-
cal strength of specimens by comparing the graphs obtained in testing
various types of steel or metals and their alloys.

The problem of measuring the specimen's vibration period, as
well as that of signaling the arrival of the moment that corresponds
to the preset value of the period are solved by the measuring-signal-
ing unit. A block diagram of the above unit is given in Fig. 6.

This unit consists of four fundamental assemblies: a measuring-
pulse shaper (UO, BT, SZ and SO), a relay for automatic triggering
of readings (RS), an MSK-2 type millisecond counter and a signaling
device (U1, U2, U3, U4, R1, R2, R3, R4 and Z).

The measuring-pulse shaper, triggering relay and millisecond
counter constitute the actual system for periodic measurement of the
vibration period. The periodicity of the measurements may be varied

in the range from 5 to 30 seconds.

In the given system, the clipper-amplifier (UO) acts as a measuring pulse shaper whose sequence time corresponds to the period of a complete vibration of the specimen.

The binary trigger (BT) separates the measuring pulses for starting and stopping period variation.

The time relay (RS) determines the time between two measurements and effects automatic triggering of the millisecond-counter readings (MSK-2).

The signaling system consisting of four amplifiers (U1, U2, U3 and U4) and relays (R1, R2, R3 and R4), employs the voltage drop across the loads on the millisecond-counter decade tubes on firing.

Operation of the four relays leads to closing of their contacts and actuation of the bell (Z).

The present apparatus enables us to measure and signal the magnitude of the period with an accuracy to $\pm 10^{-4}$ seconds; this makes it possible to analyze the smallest changes in the specimen.

REFERENCES

1. Ya. B. Fridman, Mekhanicheskiye svoystva metallov [Mechanical Properties of Metals], 1946.

2. A. Kh. Kotrell, Dislokatsii i plasticheskoye techeniye v kristallakh [Dislocations and Plastic Flow in Crystals], Izd-vo inostr. lit-ry [Foreign Literature Publishing House], 1958.

3. V. I. Likhtman, P. A. Rebinder and G. V. Karpenko, Vliyaniye poverkhnostno-aktivnoy sredy na protsessy deformatsii metallov. Izd-vo AN SSSR [Effect of Surface-Active Medium on Deformation Processes in Metals. Publishing House of the Acad. Sci. USSR, 1954.

4. L. A. Glikman, Korrozionno-mekhanicheskaya prochnost' metallov [Corrosion Mechanical Strength of Metals], 1955.

Manu-script Page No.	[List of Transliterated Symbols]
46	заз = zaz = zazor = gap
47	Д = D = datchik = sensor
47	УН = UN = usilitel' napryazheniya = voltage amplifier
47	УМ = UM = usilitel' moshchnosti = power amplifier
47	ЭМ = EM = elektromagnit = electromagnet
47	Я = Ya = yakor' = armature
47	О = O = obrazets = specimen
48	ж = zh = zhelezo = iron
50	УО = UO = usilitel'-ogranichitel' = clipper-amplifier
50	БТ = BT = binarnyy trigger = binary trigger
50	РС = RS = rele sbrosa = triggering relay
51	У = U = usilitel' = amplifier
51	Р = R = rele = relay
51	З = Z = zvonok = bell

INFLUENCE OF TEMPERATURE AND TECHNOLOGICAL FACTORS
ON THE ENDURANCE OF THERMAL-SHOCK-RESISTING STEELS AND ALLOYS

B.I. Aleksandrov

Failure of the most heavily loaded components of steam and gas
turbines operating under elevated temperature conditions are basically
fatigue in nature. The fatigue resistance of these components is one
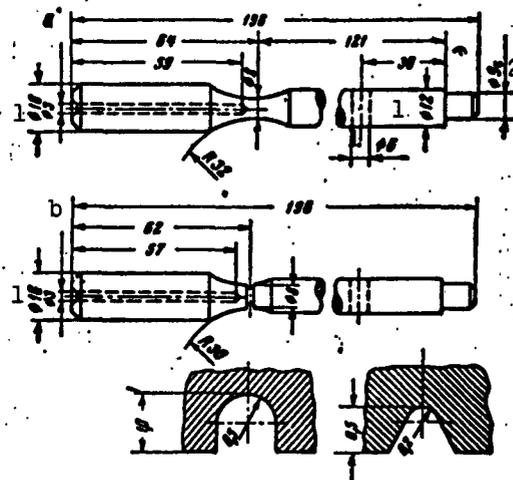
Fig. 1. Specimens used for fatigue
tests. a) Smooth; b) with circular
notch.

of the most important characteristics which must be considered in
selection of the material, the method of producing blanks, the heat-
treatment and finishing operations, as well as the methods of in-
creasing the erosion and corrosion resistance of the components.

Investigations of the endurance and sensitivity to stress con-
centration on a total of 19 heat-resistant and thermal-shock resis-
tant steels and alloys have been carried out with the participation

of I.A. Oding, I.V. Kudryavtsev, A.P. Shishkova, L.I. Savko, B.I. Aleksandrov et al. in the Strength Division of TsNIITMASh in the period from 1948 up to the present time.

Tests were conducted on a type Ya8 machine designed by S.I. Yatskevich for alternating circular bending in an air medium on bases from 30 to 300 million cycles, but mostly on a base of 100 million cycles (or 600 hours), at a frequency of approximately 3000 cycles/min and temperatures to 800°. Smooth specimens with weak-section diameters of 10 mm and specimens with a circular notch (Fig. 1) were tested. We used specimens with two types of notches: $\rho = 0.2$ mm, $t = 0.5$ mm and $\rho = 0.5$ mm, $t = 1.0$ mm. The notches were cut with either a cutting tool or a grinding wheel 1 mm thick, which was dressed to a radius of 0.5 mm. The smooth specimens were ground in the zone of greatest sectional stress with a radial-feed profile wheel.

The values of the actual endurance limit in the absence (or in the presence) of stress concentration and the sensitivity to stress concentration were determined.

Form of Endurance Curve

With a small increase in test temperature (for ferritic steels to $300-400^\circ$ and austenitic steels to $550-600^\circ$), the form of the endurance curves is the same as that at room temperature, i.e., the curve (in semilogarithmic coordinates of stress versus the logarithm of the number of cycles) consists of two rectilinear branches: one (corresponding to overloads) is sloped and the second parallel to the axis of cycles. At these temperatures, steels have a true endurance limit, i.e., a stress below which fatigue failure is practically impossible.

The first branch of the fatigue curve inclines more gently with increasing test temperature, while the second acquires an inclination

to the cycle axis; as a result of this, the angle between the branches
of the curve diminishes and many of the materials tested have fatigue
curves in the form of a single line at relatively high temperatures.
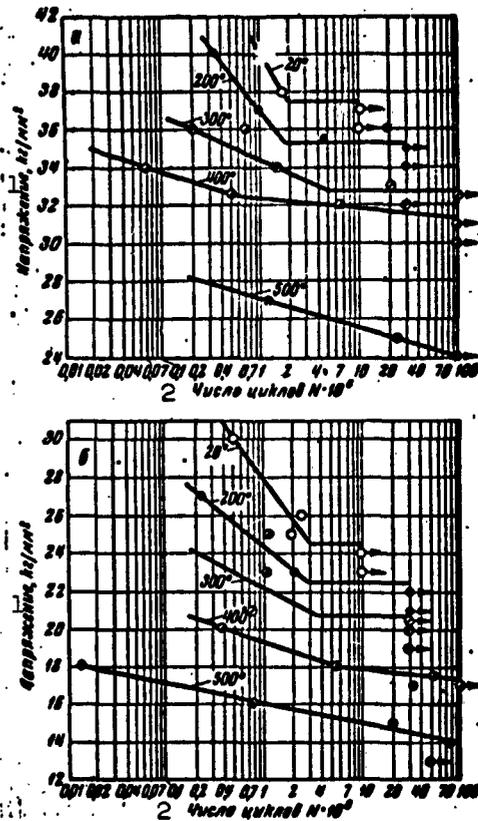
Fig. 2. Fatigue curves of 2Kh13
steel at temperatures from 20
to 500°. a) Smooth specimens;
b) specimens with ground notch,
ρ = 0 mm and t = 1.0 mm. 1)
Stress, kg/mm^{2}; 2) number of
cycles N·10^{6}.

Such a type of change in the en-
durance curves with a temperature
rise may be traced on 2Kh13 steel
(Fig. 2) when an endurance curve
in the form of a straight line is
obtained even at 500°. Similar
lines are also obtained in testing
austenitic steels and the alloys
EI-395 (at 800°), EI-437 (at 700°)
and EI-673 (at 750°).

We may assume that the ob-
jective existence of two different
relationships for number of cycles
prior to failure as a function of
stress at the operating tempera-
tures (the two branches on the en-
durance curve) is due to the radi-
cal difference in the phenomena
which take place in metal under
heavy and light overloading. Under
heavy overloads, a failure similar
to that at room temperature sets in after considerable plastic de-
formation as a result of plasticity depletion and development of kind
II and III stresses. In this case, mechanical aging, which increases
the strength and decreases the plasticity of the metal, may be another
supplementary phenomenon, while stress relaxation should not be sub-

stantial as a result of the short period preceding failure.

In cases of failures under light overloads corresponding to a large number of cycles prior to failure, plastic deformations are so small that they are in no way capable of causing failure; here the relaxation of nascent stresses may also make itself felt; this should postpone the onset of failure.

Emergence of fatigue cracks under these conditions may be the result of the action of the medium, which gives rise to wedge-shaped surface inclusions acting as stress concentrators. Moreover, softening of the metal may be caused by coagulation of the disperse phases. Certain data have been obtained in this direction. Up to the present time, however, the physical nature of the phenomena taking place in metal under cyclical loading and elevated temperature conditions is not altogether clear.

The appearance of a slope on the second branch of the endurance curves makes it necessary (for increasing the reliability of the data) to increase the test base, i.e., the maximum number of cycles that a specimen can endure without failure. In view of this, a base of 10 to 30 million cycles was used as a rule in all investigations for relatively low temperatures, while 50-100 million cycles were employed as a base at temperatures when failures are expected after prolonged periods of testing. Occasional tests were made on a base of 300 million cycles and greater.

The slopes of the fatigue curves in the region of light overloads and large number of cycles indicate the possibility of component fatigue failure on prolonged operation. In view of this, the necessity of taking this phenomenon into account arises in extending the data obtained in a relatively short-term testing process to a considerably longer period or a larger number of cycles of component operation.

If we assume that the slope of the curve obtained in the testing process does not change with further increase in the number of cycles, a conventional endurance limit for any set number of cycles may be determined either by graphic extrapolation or from the equation

$$\sigma_1 = \sigma_0 + \lg\left(\frac{N_0}{N_1}\right)^k,$$
(1)

where σ_0 and N_0 are the coordinates of the point of inflection on the endurance curve, σ_1 is the conventional endurance limit for a set number of cycles N_1, and $\underline{k}$ is a coefficient characterizing the slope of the curve.

However, the possibility of this extrapolation should be confirmed by tests on more protracted bases. In relation to this, interest is drawn to the investigations of EI-405 steel at a temperature of 500° and one billion cycles which were conducted by A.P. Shishkov. In this study, the last specimen was tested for 250 days, while obtaining of the entire curve required approximately one year.

The test showed that the slope of the endurance curve does not remain constant on increasing the test period, but may decrease, and therefore the data obtained on a base of 100 million cycles will be somewhat on the low side.

It is much more difficult to extrapolate the data obtained on a base of 100 million cycles for a significantly larger number of cycles or prolonged operating time of the component than might be assumed at first glance. This is associated with the difficulty of determining the slope of the endurance curve at the operating temperature in the region of small overloads. Accurate determination of the slope is made difficult by the small number of experimental points that refer to the second branch of the curve and due to possible scattering of the durability values for these points. The test time (machine-hours) for one series of specimens should increase by several times when,

- 56 -
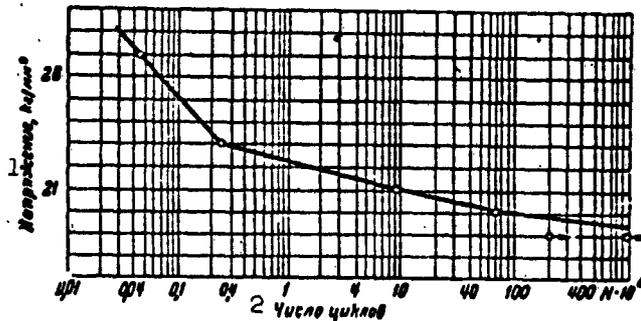
Fig. 3. Fatigue curves of EI-405 steel at
500°. Specimens with spot [sic; machined]
circular notches $\rho = 0.5$ mm, $t = 1.0$ mm.
1) Stress, kg/mm^2; 2) number of cycles.

besides the conventional endurance limit, the slope of the curve in
the region of minor overloads must be determined.

Interest is also drawn to data relating to the influence of the
type of stressed state on the path of the fatigue curve in order to
establish the possibility of extrapolating the results of fatigue
tests. In relation to this, comparison of fatigue curves obtained
from testing smooth specimens with similar curves for notched speci-
mens, in whose surface layers, as we know, a two-dimensional stress
(biaxial tension or compression) is produced on bending, may be found
useful. In the majority of cases, these curves run parallel for ma-
terials in a relatively stable state (after quenching and stabiliza-
tion), while the breaking points correspond to one and the same number
of cycles. Differences in curve path may be observed for less stable
states. This occurs, for example, in the case of EI-123 steel at 550°
when the fatigue curve of notched specimens has a slope in the region
of large numbers of cycles, while a second branch of the curve was
obtained parallel to the axis of cycles for notchless specimens.

Influence of Temperature on Endurance Limit

Figure 4 shows the variation in the conventional endurance limit

- 57 -

of ferrite-based steels. With the general tendency to significant
lowering of the conventional endurance limit of these steels with a
rise in temperature, a delay in the endurance drop (1Kh13, 2Kh13
and EI-755) is observed in the temperature region from 300 to 400°.
In this temperature region, certain steels even show an increase in
endurance limit (30KhM and EI-723). A sharp drop in the endurance
limit of ferrite steels occurs at test temperatures elevated above
400-500°.
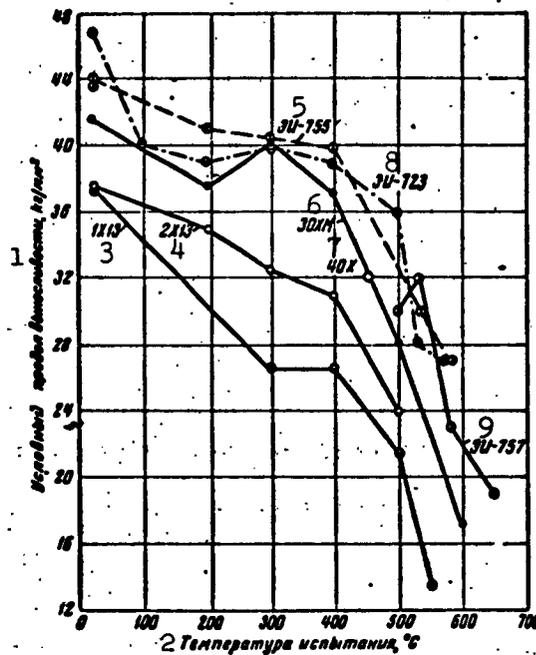
Fig. 4. Dependence of actual en-
durance limits of thermal-shock re-
sisting ferrite steels upon test
temperature (smooth specimens after
improvement). 1) Conventional en-
durance limit, kg/mm^2; 2) test tem-
perature, °C; 3) 1Kh13; 4) 2Kh13;
5) EI-755; 6) 30KhM; 7) 40Kh; 8)
EI-723; 9) EI-757.

The fatigue resistance of semiferrite steels is dependent to a
major degree upon carbon content and presence of alloying elements.
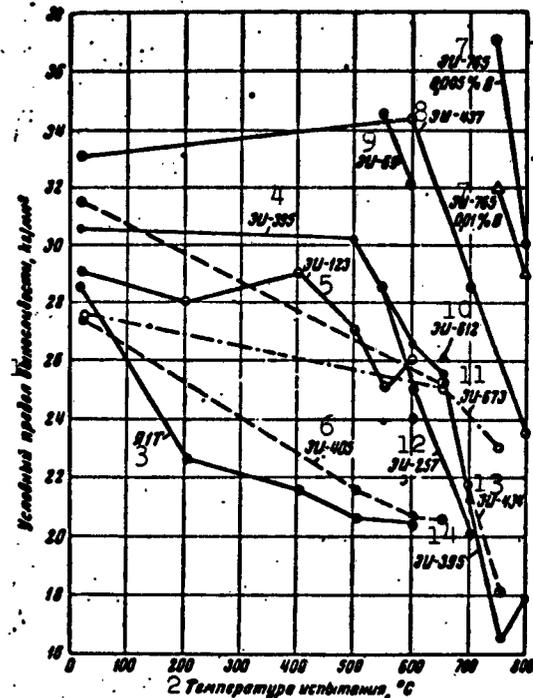
Fig. 5. Dependence of conventional
endurance limits of heat-resisting
austenitic steels and alloys upon
test temperature. 1) Conventional
fatigue resistance, kg/mm^2; 2) test
temperature, $°C$; 3) YalT; 4) EI-
395; 5) EI-123; 6) EI-405; 7) EI-
765; 8) EI-437; 9) EI-69; 10) EI-
612; 11) EI-673; 12) EI-257; 13)
EI-434; 14) EI-395.

The greater the carbon content, the greater will be the fatigue re-
sistance; this is indicated by the fact that the fatigue resistance
of 2Kh13 steel is greater than that of 1Kh13 steel.

Complex alloying with molybdenum, vanadium, tungsten and other
elements exerts a particularly favorable influence on the fatigue re-
sistance of ferrite steels. Among the ferrite-based steels, the
stainless steels EI-755 and EI-757 and the compound-alloy pearlite
steel EI-723 possess the highest conventional endurance limits in the
temperature range from room temperature even up to $580°$.

It is interesting to note that the reduction in the conventional endurance limits of EI-755, EI-757 and EI-723 steels has approximately the same character in the temperature range from 400 to 535° in spite of the large difference in their corrosion resistance.

The advantages of EI-755 and EI-757 stainless steels over EI-723 pearlitic steel should no doubt have appeared in prolonged test periods, since it was already established by tests on a base of 100 million cycles (600 hours) that failure of EI-723 steel is corrosion-fatigue in nature at temperatures of 500° and above, while corrosive action is not noted in EI-755 and EI-757 steels even at a temperature of 580°.

At 500°, the majority of austenitic steels have a conventional endurance limit approximately the same as that at 20° (Fig. 5).

The steels and alloys may be arranged in the following manner in order of increasing restricted endurance limit at $600-650^{\circ}$: YalT, EI-405, EI-257, EI-395, EI-434, EI-612, EI-673, EI-69 and EI-437. The presence of large quantities of disperse carbide or intermetalloid components exerts a decisive influence on the fatigue resistance of steels (with an austenitic basic solid solution) at temperatures of $600-700^{\circ}$. Thus, for example, as compared with EI-257 steel, EI-69 steel showed high fatigue resistance due to simultaneously high carbon and tungsten contents.

The conventional endurance limit of EI-434, EI-395 and EI-673 steels are approximately the same ($24-26$ kg/mm^2) at 650°. Differences between these three steels appear at higher temperatures when the extent to which the fundamental solid solution is alloyed with nickel, chromium and cobalt begins to play the major role. The most heavily alloyed metal, EI-765, possesses maximum fatigue resistance at 750°; alloy EI-765 and the steels EI-673, EI-434 and EI-395 follow there-

after in order of decreasing resistance.

A composite endurance diagram of ferrite- and austenite-based materials is given in Fig. 6.

The high-alloy stainless steels EI-755 and EI-757 and the pearlite steel EI-723 have conventional limits above those of the medium-alloy austenitic EI-257, EI-123 and other steels at temperatures up to and including 535°. At 580°, the conventional endurance limit of EI-755 steel is approximately the same as that of medium-alloy austenitic steels. Steels and alloys that are based on austenite have higher endurance at temperatures above 580°.

At 650 and 700°, cast austenitic steels have somewhat lower endurance limits than do forged austenitic steels of similar composition.

Type EI-765 chromium-nickel-based alloy showed particularly outstanding properties in the 750-to-800° temperature region. Its conventional endurance limit at 750 and 800° exceeds by far the values for other high-alloy heat-resisting steels and alloys that we tested.

A comparison of the endurance limits in the presence of stress concentration for various groups of metals (ground notches) is given in Fig. 7, where the advantages of ferrite steels at relatively low temperatures — to 400° — and high-alloy ferrite EI-755 and EI-757 steels to 535° are seen. The endurances of these ferritic and austenitic steels coincide at 580°, while the advantages are on the side of the austenitic steels at higher temperatures.

It is interesting to compare sensitivities to stress concentration. Maximum sensitivity is frequently observed at temperatures of approximately 200-300° for ferrite steels (35KhM and EI-723). It is found that the stainless heat-resisting materials EI-755 and EI-757, while possessing high endurance limits, are, at the same time, extremely sensitive to stress concentration ($q = 0.8$ rather than 0.4-

- 61 -

0.6 for 1Kh13 and 2Kh13). Like ferrite materials, austenitic steels are also sensitive to stress concentration at room and operating temperatures; however, alloy EI-765 showed low sensitivity to stress concentration (q = 0.3-0.4), together with high endurance at operating temperatures of 750 and 800°.
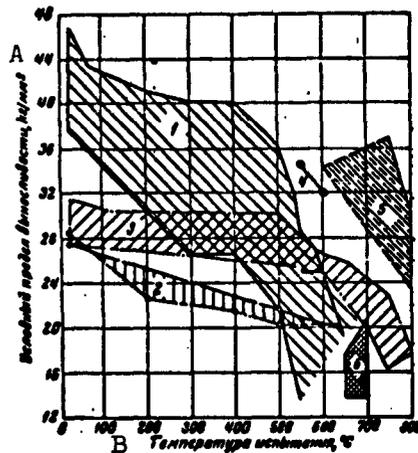
Fig. 6. Dependence of conventional endurance limits of steels and alloys upon test temperature. 1) Thermal-shock and heat-resisting ferrite steels; 2) stable EI-405 and EYalT austenitic steels; 3) austenitic steels with considerable quantity of elements that increase heat resistance; 4) EI-69 austenitic steel; 5) heat-resisting chromium-nickel-based alloys; 6) cast austenitic steels. A) Conventional endurance limit, kg/mm^2; B) test temperature, $°C$.
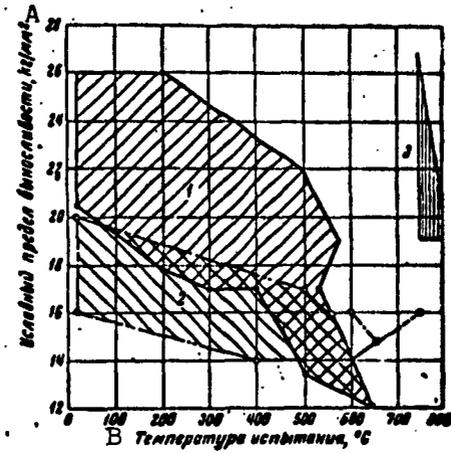
Fig. 7. Dependence of conventional endurance limits of steels and alloys upon test temperature in presence of stress concentrators. 1) Thermal-shock and heat-resisting ferrite steels; 2) austenitic steels; 3) alloy EI-765. A) Conventional endurance limit, kg/mm^2; B) test temperature, $°C$.

Influence of Heat Treatment, Casehardening and Plastic Deformation on Endurance Limit

An increase in the quenching temperature of EI-757 steel from 1050 to 1150° with three-hour tempering to 680° enables us to increase the conventional endurance limit at 580° without stress concentration by 6 kg/mm^2 (or 26%) and by 2 kg/mm^2 (or 11%) with stress concentra-

tion. Change in the stabilization procedure of EI-434 and EI-395 steels does not exert a substantial influence on endurance. The endurance limit for EI-434 steel at 650° is at a level of 21-22 kg/mm^2 without stress concentrators and after various stabilization procedures, while it is at a level of 14.5-17 kg/mm^2 with stress concentration. The same is also observed for EI-395 steel at 650°; change in the stabilization procedure of this steel exerts hardly any influence whatever on its endurance limit without concentrators.

In view of the development of new case-hardening processes for such heavily loaded components as rotor blades (for the purpose of increasing their erosion resistance), interest is attracted to the problem of the influence of these treatments on the fatigue-resistance characteristics of the materials. Investigations conducted up to this time have established that chromizing in an ammonium iodide medium at 1050° for 10 hours with subsequent high-temperature nitriding or cyaniding combined with heating for quenching, while increasing erosion resistance, at the same time increases the fatigue resistance of EI-405 steel at 600°.

Aluminum-chromium plating as well as spark-discharge machining of EI-434 steel decreases its endurance. A reduction in endurance is also obtained after aluminum-chromium plating or after carburizing and chromium plating of EI-612 steel. The above data indicate that treatments which increase erosion resistance may, at the same time, affect the fatigue resistance of the components in different ways.

It has been established as a result of study of the influence of continuous deformation (tensioning at room and elevated temperatures, torsion, and compression in die blocks under a hammer) on the endurance and sensitivity to stress concentration of six austenitic steels (EI-257, EYaIT, EI-405, EI-395, EI-434 and EI-69) at $580-650^\circ$ that

- 63 -

continuous deformation may give rise to either an increase or decrease in the endurance of austenitic steels at elevated temperatures. A positive effect of this deformation is more probable for structurally stable steels (for example, EI-257 and EI-405) in deformation under mild stress conditions (for example, biaxial compression), with moderate amounts of plastic deformation, which are different for different steels and stressed states, and in deformation under room-temperature conditions.

A negative effect of continuous work hardening is more probable for structurally unstable steels which show higher hardness on heating (for example, EI-69) in deformation under rigid stress conditions (for example, tension), with large amounts of plastic deformation and in deformation under elevated temperature conditions.

Investigation of the influence of surface hardening (shotblast work hardening and surface rolling) on the endurance and sensitivity to stress concentration of steels with a sorbite structure (30KhM, 1Kh13, 2Kh13 and EI-723) at temperatures to 535° enabled us to establish that surface work hardening of these steels effects a 10-25% increase in the endurance limit at operating temperatures in cases without stress concentration and a 40-90% increase with stress concentrators. The effect of shot blasting and surface rolling on the endurance of 2Kh13 steel is shown as an example in Fig. 8.

Surface work hardening (surface rolling) of austenitic steels, which is carried out after quenching, increases the endurance limit at operating temperatures ($600-650^{\circ}$) by 11-33% without stress concentration and 31-63% with concentrators. The hardening effect is retained at both operating and above-operating temperatures (Fig. 9). The steels under study may be arranged as follows in order of increas-

ing effect of surface work hardening: EI-123, EI-434, EI-395, EI-673 and EI-405. The effectiveness of surface work hardening is greater where it is accomplished after quenching and prior to stabilization, but not after completion of the final heat treatment (Fig. 10).
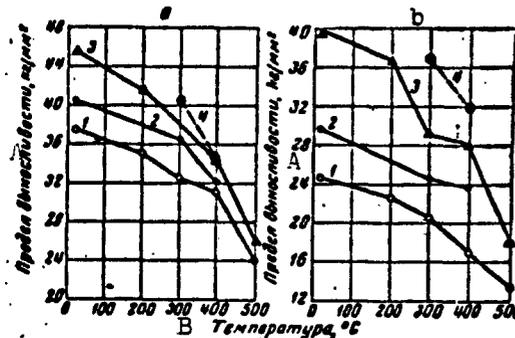
Fig. 8. Dependence of conventional endurance limits of smooth (a) and notched (b) 2Kh13 steel specimens upon temperature (quenching from 1050° in oil and tempering at 700° for 3 hours). 1) Without surface hardening; 2) shotblast work hardening and polishing; 3) surface rolling; 4) surface rolling and holding for 750 hours at test temperature.
A) Endurance limit, kg/mm^2; B) temperature, °C.

In many cases, reduction in the endurance of components, which is caused by the effect of stress concentrators in the form of notches, grooves or joints with negative allowance is avoided altogether with surface work hardening.

The favorable residual stresses and hardening of the surface layers of metal obtained after quenching, surface work hardening and stabilization are stable under the prolonged action of operating temperatures and cyclical loading.

Surface work hardening may change the nature of the precipitating phases on subsequent aging (for example, eliminate the ferromagnetic phase in EI-434 steel from the grain boundaries and from

- 65 -
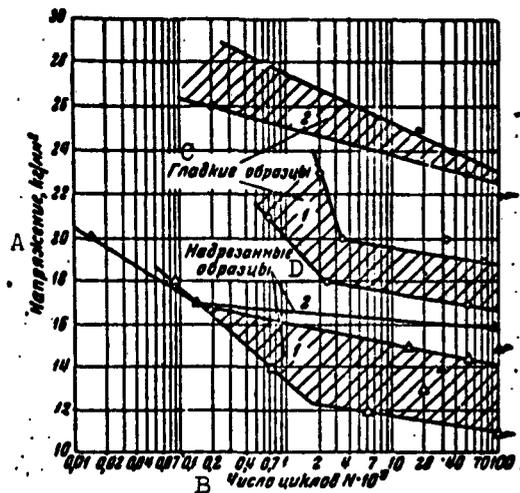
Fig. 9. Fatigue curves of EI-395
steel at 750°. 1) Quenching at
1180° and stabilization (650°,
100 hours + 800°, 10 hours); 2)
quenching at 1180°, surface roll-
ing and stabilization (650°, 100
hours + 800°, 10 hours). A) Stress,
kg/mm^2; B) number of cycles $N \cdot 10^6$;
C) smooth specimens; D) notched
specimens.
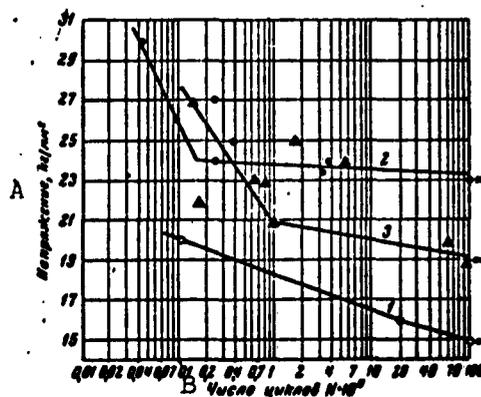
Fig. 10. Fatigue curves of EI-673
steel at 650° (specimens with ground
circular notch $\rho = 0.5$, $t = 1.0$ mm).
1) Quenching in oil at 1200° and sta-
bilization (760°, 70 hours); 2) quench-
ing in oil at 1200°, surface rolling
and stabilization (760°, 24 hours); 3)
quenching in oil at 1200°, stabiliza-
tion (760°, 70 hours), surface rolling
and stabilization (650°, 50 hours). A)
Stress, kg/mm^2; B) number of cycles $N \cdot 10^6$.

around the primary carbides), as well as the nature of the effect
of the ambient medium by changing nonuniform medium activity into
uniform activity without formation of wedge-shaped inclusions along
grain boundaries, which may chip and act as seats of fatigue failure
and thereby reduce endurance.

Manu-
script   [List of Transliterated Symbols]
Page
No.

53   ЦНИИТМАШ = TsNIITMASh = Tsentral'nyy nauchno-issledovatel'skiy
                     institut tekhnologii i mashin = Central
                     Scientific Research Institute of Technology
                     and Machinery

REFERENCES

1. S.I. Yatskevich, Mashina dlya ispytaniya nepodvizhnogo obraztsa na ustalost' pri povyshennykh temperaturakh [Machine for Testing Stationary Specimens for Fatigue at Elevated Temperatures], "Zavodskaya laboratoriya" [Industrial Laboratory], No. 1, 1949.

2. I.V. Kudryavtsev and L.I. Savko, Issledovaniye ustalostnoy prochnosti spetsial'nykh staley pri vysokikh temperaturakh [Investigation of the Fatigue Strength of Special Steels at High Temperatures], Sb. TsNIITMASh [Collection of Central Scientific Research Institute for Technology and Machinery], "Ustalostnaya prochnost' stali" [Fatigue Strength of Steels], Mashgiz [State Scientific and Technical Publishing House of Literature on Machinery], Book 43, 1951.

3. I.A. Oding and A.P. Shishkova. Vliyaniye stareniya i naklepa na ustalostnuyu prochnost' austenitnykh staley pri vysokikh temperaturakh [Influence of Aging and Cold Working on the Fatigue of Austenitic Steels at High Temperatures], "Vestnik mashinostroyeniya" [Herald of Machine Building], No. 6, 1954.

4. B.I. Aleksandrov. Issledovaniye ustalostnoy prochnosti dvukh splavov pri povyshennykh temperaturakh [Investigation of the Fatigue Strength of Two Alloys at High Temperatures], Sb. TsNIITMASh, "Konstruktsionnaya prochnost' staley [Structural Strength of Steels], Book 63, Mashgiz [State Scientific and Technical Publishing House of Literature on Machinery], 1954.

5. A.P. Shishkova, Vysokotemperaturnyye ispytaniya pri odnom milli-

- 68 -

arde tsiklov [High-Temperature Tests With One Billion Cycles],
Sb. TsNIITMASh, "Voprosy konstruktsionnoy prochnosti stali"
[Problems of the Structural Strength of Steel], Book 85, Mashgiz
[State Scientific and Technical Publishing House of Literature
on Machinery], 1957.

6. I.V. Kudryavtsev and B.I. Aleksandrov, Vliyaniye poverkhnostnogo
naklepa na ustalostnuyu prochnost' stali 2Kh13 pri povyshennykh
temperaturakh [Influence of Surface Hardening on the Fatigue
Strength of Steel 2Kh13 at High Temperatures], "Teploenergetika"
[Heat Engineering], No. 7, 1954.

7. B.I. Aleksandrov, Ustalost' stali EI-723 pri vysokikh temperaturakh
[Fatigue of Steel EI-723 at High Temperatures], "Metallovedeniye
i obrabotka metallov" [Metallography and Metalworking], No. 12,
1956.

8. B.I. Aleksandrov, A.P. Shishkova. Vliyaniye otpuska i poverkhnost-
nogo uprochneniya na ustalostnuyu prochnost' stali EI-434 pri
povyshennykh temperaturakh [Influence of Tempering and Surface
Hardening on the Fatigue Strength of Steel EI-434 at High
Temperatures], Sb. TsNIITMASh "Voprosy konstruktsionnoy prochnosti
stali" [Problems of the Structural Strength of Steel], Book 85,
Mashgiz [State Scientific and Technical Publishing House of
Literature on Machinery], 1957.

9. I.V. Kudryavtsev and B.I. Aleksandrov, Ustalostnaya prochnost'
stali 1Kh13 pri vysokikh temperaturakh na obraztsakh s nepovizh-
nymi soyedineniyami [Fatigue Strength of Steel 1Kh13 at High
Temperatures in Specimens with Fixed Joints], [Affiliate of
VINITI (not identified)], Report No. M-58-391/4, 1958.

10. I.V. Kudryavtsev and B.I. Aleksandrov, Vliyaniye naklepa na
vynoslivost' zharoprochnykh i teploustoychivykh staley pri

- 69 -

vysokikh temperaturakh [Influence of Cold Working on the Endurance of Heat- and Thermal-Shock-Resistant Steels at High Temperatures], Sb. TBTItyazhmash [Collection of Central Office of Technical Inrormation on Heavy Machinery], "Uprochneniye poverkhnostnym naklepom" [Surface Hardening by Cold Working], Book 52-5, Moscow, 1958.

11. B.I. Aleksandrov, Vynoslivost' austenitnoy stali EI-123 pri povyshennykh temperaturakh [Endurance of Austenitic Steel EI-123 at High Temperatures], Trudy TsNIITMASh [Transactions of Central Scientific Research Institute of Technology and Machinery], No. 2, 1959.

- 70 -

DISTRIBUTION LIST

DEPARTMENT OF DEFENSE	Nr. Copies	MAJOR AIR COMMANDS	Nr. Copies
		AFSC	
		SCFDD	1
		DDC	25
		TDBTL	5
HEADQUARTERS USAF		TDBDP	2
		AEDC (AEY)	1
AFCIN-3D2	1	ASD (ASYIM)	2
ARL (ARB)	1		

OTHER AGENCIES

CIA	1
NSA	6
DIA	9
AID	2
OTS	2
AEC	2
PWS	1
NASA	1
ARMY (FSTC)	3
NAVY	3
NAFEC	1
RAND	1
AFCRL (CRXLR)	1
SPECTRUM	1